A&A 577, A128 (2015)
DOI: 10.1051/0004-6361/201525803

Astronomy & Astrophysics

CARMENES input catalogue of M dwarfs

I. Low-resolution spectroscopy with CAFOS⋆

F. J. Alonso-Floriano[1], J. C. Morales[2,3], J. A. Caballero[4], D. Montes[1], A. Klutsch[5,1], R. Mundt[6], M. Cortés-Contreras[1], I. Ribas[2], A. Reiners[7], P. J. Amado[8], A. Quirrenbach[9], and S. V. Jeffers[7]

[1] Departamento de Astrofísica y Ciencias de la Atmósfera, Facultad de Ciencias Físicas, Universidad Complutense de Madrid, 28040 Madrid, Spain
e-mail: fjalonso@fis.ucm.es
[2] Institut de Ciències de l'Espai (CSIC-IEEC), Campus UAB, Facultat Ciències, Torre C5 – parell – 2ª, 08193 Bellaterra, Barcelona, Spain
[3] LESIA-Observatoire de Paris, CNRS, UPMC Univ. Paris 06, Univ. Paris-Diderot, 5 Pl. Jules Janssen, 92195 Meudon Cedex, France
[4] Departamento de Astrofísica, Centro de Astrobiología (CSIC–INTA), PO Box 78, 28691 Villanueva de la Cañada, Madrid, Spain
[5] INAF−Osservatorio Astrofisico di Catania, via S. Sofia 78, 95123 Catania, Italy
[6] Max-Planck-Institut für Astronomie, Königstuhl 17, 69117 Heidelberg, Germany
[7] Institut für Astrophysik, Friedrich-Hund-Platz 1, 37077 Göttingen, Germany
[8] Instituto de Astrofísica de Andalucía (CSIC), Glorieta de la Astronomía s/n, 18008 Granada, Spain
[9] Landessternwarte, Zentrum für Astronomie der Universität Heidelberg, Königstuhl 12, 69117 Heidelberg, Germany

Received 4 February 2015 / Accepted 18 February 2015

ABSTRACT

Context. CARMENES is a stabilised, high-resolution, double-channel spectrograph at the 3.5 m Calar Alto telescope. It is optimally designed for radial-velocity surveys of M dwarfs with potentially habitable Earth-mass planets.
Aims. We prepare a list of the brightest, single M dwarfs in each spectral subtype observable from the northern hemisphere, from which we will select the best planet-hunting targets for CARMENES.
Methods. In this first paper on the preparation of our input catalogue, we compiled a large amount of public data and collected low-resolution optical spectroscopy with CAFOS at the 2.2 m Calar Alto telescope for 753 stars. We derived accurate spectral types using a dense grid of standard stars, a double least-squares minimisation technique, and 31 spectral indices previously defined by other authors. Additionally, we quantified surface gravity, metallicity, and chromospheric activity for all the stars in our sample.
Results. We calculated spectral types for all 753 stars, of which 305 are new and 448 are revised. We measured pseudo-equivalent widths of Hα for all the stars in our sample, concluded that chromospheric activity does not affect spectral typing from our indices, and tabulated 49 stars that had been reported to be young stars in open clusters, moving groups, and stellar associations. Of the 753 stars, two are new subdwarf candidates, three are T Tauri stars, 25 are giants, 44 are K dwarfs, and 679 are M dwarfs. Many of the 261 investigated dwarfs in the range M4.0–8.0 V are among the brightest stars known in their spectral subtype.
Conclusions. This collection of low-resolution spectroscopic data serves as a candidate target list for the CARMENES survey and can be highly valuable for other radial-velocity surveys of M dwarfs and for studies of cool dwarfs in the solar neighbourhood.

Key words. stars: activity – stars: late-type – stars: low-mass

1. Introduction

The Calar Alto high-Resolution search for M dwarfs with Exo-earths with Near-infrared and optical Échelle Spectrographs (hereafter CARMENES[1]) is a next-generation instrument close to completion for the Zeiss 3.5 m Calar Alto telescope, which is located in the Sierra de Los Filabres, Almería, in southern Spain, at a height of about 2200 m (Sánchez et al. 2007, 2008). CARMENES is the name used for the instrument, the consortium of 11 German and Spanish institutions that builds it, and of the scientific project to be carried out during guaranteed time observations. The instrument consists of two separated, highly stable, fibre-fed spectrographs covering the wavelength ranges from 0.55 to 0.95 μm and from 0.95 to 1.70 μm at spectral resolution $R \approx 82\,000$, each of which shall perform high-accuracy radial-velocity measurements with long-term stability of $\sim$1 m s^{-1} (Quirrenbach et al. 2010, 2012, 2014, and references therein; Amado et al. 2013). First light is scheduled for the summer of 2015, followed by the commission of the instrument in the second half of that year.

The main scientific objective for CARMENES is the search for very low-mass planets (i.e., super- and exo-earths) orbiting mid- to late-M dwarfs, including a sample of moderately active M-dwarf stars. Dwarf stars of M spectral type have effective temperatures between 2300 and 3900 K (Kirkpatrick et al. 2005; Rajpurohit et al. 2013). For stars with ages greater than

⋆ Full Tables A.1, A.2, and A.3 are only available at the CDS via anonymous ftp to cdsarc.u-strasbg.fr (130.79.128.5) or via http://cdsarc.u-strasbg.fr/viz-bin/qcat?J/A+A/577/A128

[1] http://carmenes.caha.es – Pronunciation: /kαr'·mεn·εs/

that of the Hyades, of about 0.6 Ga, these effective temperatures translate in the main sequence into a mass interval from 0.09 to 0.55 $M_\odot$, approximately (Baraffe et al. 1998; Chabrier et al. 2000; Allard et al. 2011). Of particular interest is the detection of very low-mass planets in the stellar habitable zone, the region around the star within which a planet can support liquid water (Kasting et al. 1993; Joshi et al. 1997; Lammer et al. 2007; Tarter et al. 2007; Scalo et al. 2007). In principle, the lower the mass of a host star, the higher the radial-velocity amplitude velocity induced (i.e., $K_{\rm star}$ is proportional to $M_{\rm planet}\, a^{-1/2}$ $(M_{\rm star} + M_{\rm planet})^{-1/2} \approx (a\, M_{\rm star})^{-1/2}$ when $M_{\rm star} \gg M_{\rm planet}$). In addition, the lower luminosity of an M dwarf with respect to a star of earlier spectral type causes its habitable zone to be located very close to the host star, which makes detecting habitable planets around M dwarfs (at ∼0.1 au) easier than detections around solar-like stars (at ∼1 au).

From transit surveys with the NASA 0.95 m *Kepler* space observatory, very small planet candidates are found to be relatively more abundant than Jupiter-type candidates as the host stellar mass decreases (Howard et al. 2012; Dressing & Charbonneau 2013, 2015; Kopparapu 2013; Kopparapu et al. 2013). For early-M dwarf stars in the field, some radial-velocity studies have already been carried out (ESO CES, UVES and HARPS by Zechmeister et al. 2009, 2013; CRIRES by Bean et al. 2010; HARPS by Bonfils et al. 2013), but the much-sought value of $\eta_\oplus$, that is, the relative abundance of Earth-type planets in the habitable zone, is as yet only poorly constrained from radial-velocity data (e.g., $\eta_\oplus = 0.41^{+0.54}_{-0.13}$ from Bonfils et al. 2013).

Highly stable, high-resolution spectrographs in the near-infrared currently under construction, such as SPIRou (Artigau et al. 2014), IRD (Kotani et al. 2014), HPF (Mahadevan et al. 2014), and CARMENES, are preferable over visible for targets with spectral types M4 V or later (see Table 1 in Crossfield 2014). This is because the spectral energy distribution of late-M dwarfs approximately peaks at 1.0−1.2 μm (Reiners et al. 2010), while HARPS and its copy in the northern hemisphere, HARPS-N, cover the wavelength interval from 0.38 to 0.69 μm. That faintness in the optical is quantitatively illustrated with the tabulated V magnitudes of the brightest M dwarfs in the northern hemisphere (HD 79210/GJ 338 A, HD 79211/GJ 338 B, and HD 95735/GJ 411) at 7.5−7.7 mag, far from the limit of the naked human eye.

The specific advantage of CARMENES is the wide wavelength coverage and high spectral resolution in both visible and near-infrared channels. Simultaneous observation from 0.5 to 1.7 μm is a powerful tool for distinguishing between genuine planet detections and false positives caused by stellar activity, which have plagued planet searches employing spectrographs with a smaller wavelength coverage, especially in the M-type spectral domain (Reiners et al. 2010; Barnes et al. 2011). A substantial amount of guaranteed time for the completion of the key project is also an asset.

A precise knowledge of the targets is critical to ensure that most of the CARMENES guaranteed time is spent on the most promising targets. This selection involves not only a comprehensive data compilation from the literature, but also summarises our observational effort to achieve new low- and high-resolution optical spectroscopy and high-resolution imaging. The present publication on low-resolution spectroscopy is the first paper of a series aimed at describing the selection and characterisation of the CARMENES sample. We have shown some preliminary results at conferences before that described the input catalogue description and selection (Caballero et al. 2013; Morales et al. 2013), low-resolution spectroscopy (Klutsch et al. 2012; Alonso-Floriano et al. 2013a), high-resolution spectroscopy (Alonso-Floriano et al. 2013b; Passegger et al. 2014), resolved multiplicity (Béjar et al. 2012; Cortés-Contreras et al. 2013), X-rays (Lalitha et al. 2012), exploitation of public databases (Montes et al. 2015), or synergies with *Kepler* K2 (Rodríguez-López et al. 2014). This first item of the CARMENES science-preparation series details the low-resolution optical spectroscopy of M dwarfs with the CAFOS spectrograph at the Zeiss 2.2 m Calar Alto telescope.

Table 1. Completeness and limiting J-band magnitudes per spectral type for the CARMENES input catalogue.

Spectral type	J [mag]	
	Completeness	Limiting
M0.0–0.5 V	7.3	8.5
M1.0–1.5 V	7.8	9.0
M2.0–2.5 V	8.3	9.5
M3.0–3.5 V	8.8	10.0
M4.0–4.5 V	9.3	10.5
M5.0–5.5 V	9.8	11.0
M6.0–6.5 V	10.3	11.5
M7.0–7.5 V	10.8	11.5
M8.0–9.5 V	11.3	11.5

2. CARMENES sample

To prepare the CARMENES input catalogue with the best targets, we systematically collected all published M dwarfs in the literature that fulfilled two simple criteria:

- They had to be observable from Calar Alto with target declinations $\delta > -23$ deg (i.e., zenith distances <60 deg, air masses at culmination <2.0).
- They were selected according to late spectral type and brightness. We only catalogued confirmed dwarf stars with an accurate spectral type determination from spectroscopic data (i.e., not from photometry) between M0.0 V and M9.5 V. Additionally, we only compiled the brightest stars of each spectral type. Our database contains virtually all known M dwarfs that are brighter than the completeness magnitudes shown in Table 1, and most of them brighter than the limiting magnitudes. No target fainter than $J = 11.5$ mag is in our catalogue.

We started to fill the CARMENES database with the M dwarfs from the Research Consortium on Nearby Stars[2], which catalogues all known stars with measured astrometric parallaxes that place them within 10 pc (e.g., Henry et al. 1994; Kirkpatrick et al. 1995; Riedel et al. 2014; Winters et al. 2015). The RECONS stellar compilation was next completed with the Palomar/Michigan State University survey catalogue of nearby stars (PMSU – Reid et al. 1995, 2002; Hawley et al. 1996; Gizis et al. 2002). Afterwards, we gave special attention to the comprehensive proper-motion catalogues of Lépine et al. (2003, 2009, 2013) and Lépine & Gaidos (2011), and the "Meeting the Cool Neighbors" series of papers (Cruz & Reid 2002; Cruz et al. 2003, 2007; Reid et al. 2003, 2004, 2008). Table 2 provides the sources of our information on M dwarfs. Until we start our survey at the

[2] http://www.recons.org

Table 2. Sources of the CARMENES input catalogue.

Source	Reference[a]	Number of stars
The Palomar/MSU nearby star spectroscopic survey	PMSU[b]	676
A spectroscopic catalog of the brightest ($J < 9$) M dwarfs in the northern sky	Lépine et al. (2013)	446
G. P. Kuiper's spectral classifications of proper-motion stars	Bidelman (1985)	285
An all-sky catalog of bright M dwarfs[c]	Lépine & Gaidos (2011)	248
Spectral types of M dwarf stars	Joy & Abt (1974)	223
Spectral classification of high-proper-motion stars	Lee (1984)	118
Meeting the cool neighbors	RECONS[d]	22
Search for nearby stars among proper... III. Spectroscopic distances of 322 NLTT stars	Scholz et al. (2005)	19
New neighbors: parallaxes of 18 nearby stars selected from the LSPM-North catalog	Lépine et al. (2009)	13
Near-infrared metallicities, radial velocities and spectral types for 447 nearby M dwarfs	Newton et al. (2014)	10

Notes. [(a)] Some other publications and meta-archives that we have searched for potential CARMENES targets are Kirkpatrick et al. (1991), Gizis (1997), Gizis & Reid (1997), Gizis et al. (2000b), Henry et al. (2002, 2006), Mochnacki et al. (2002), Gray et al. (2003), Bochanski et al. (2005), Crifo et al. (2005), Lodieu et al. (2005), Scholz et al. (2005), Phan-Bao & Bessell (2006), Reylé et al. (2006), Riaz et al. (2006), Caballero (2007, 2009, 2012), Gatewood & Coban (2009), Shkolnik et al. (2009, 2012), Bergfors et al. (2010), Johnson et al. (2010), Boyd et al. (2011), Irwin et al. (2011), West et al. (2011), Avenhaus et al. (2012), Deacon et al. (2012), Janson et al. (2012, 2014), Frith et al (2013), Jódar et al. (2013), Malo et al. (2013), Aberasturi et al. (2014), Dieterich et al. (2014), Riedel et al. (2014), Yi et al. (2014), Gaidos et al. (2014), and the DwarfArchive at `http://dwarfarchive.org`. [(b)] PMSU: Reid et al. (1995, 2002); Hawley et al. (1996); Gizis et al. (2002). [(c)] With spectral types derived from spectroscopy in this work. [(d)] RECONS: Henry et al. (1994, 2006); Kirkpatrick et al. (1995); Jao et al. (2011); Riedel et al. (2014); Winters et al. (2015) and references therein.

end of 2015, we will still include some new, particularly bright, late, single, M dwarfs[3].

As of February 2015, our input catalogue, dubbed CARMENCITA (CARMENES Cool dwarf Information and daTa Archive), contains approximately 2200 M dwarfs. For each target star, we tabulate a number of parameters compiled from the literature or measured by us with new data: accurate astrometry and distance, spectral type, photometry in 20 bands from the ultraviolet to the mid-infrared, rotational, radial, and Galactocentric velocities, Hα emission, X-ray count rates and hardness ratios, close and wide multiplicity data, membership in open clusters and young moving groups, target in other radial-velocity surveys, and exoplanet candidacy (Caballero et al. 2013). The private on-line catalogue, including preparatory science observations (i.e., low- and high-resolution spectroscopy, high-resolution imaging), will become public as a CARMENES legacy.

Of the 2200 stars, we discard all spectroscopic binaries and multiples, and resolved systems with physical or visual companions at less than 5 arcsec to our targets. The size of the CARMENES optical fibres projected on the sky is 1.5 arcsec (Seifert et al. 2012; Quirrenbach et al. 2014), and consequently any companion at less than 5 arcsec may induce real or artificial radial-velocity variations that would contaminate our measurements (Guenther & Wuchterl 2003; Ehrenreich et al. 2010; Guenther & Tal-Or 2010). About 1900 single stars currently remain after discarding all multiple systems.

2.1. CAFOS sample

The aim of our low-resolution spectroscopic observations is twofold: (i) to increase the number of bright, late-M dwarfs in CARMENCITA and (ii) to ensure that the compiled spectral types used for the selection and pre-cleaning are correct. With this double objective in mind, we observed the following:

- High proper-motion M-dwarf candidates from Lépine & Shara (2005) and Lépine & Gaidos (2011) with spectral types with large uncertainties or derived only from photometric colours. Spectral types from $V^* - J$ colours are not suitable for our purposes (Alonso-Floriano et al. 2013a; Mundt et al. 2013; Lépine et al. 2013 – V^* is an average of photographic magnitudes B_J and R_F from the Digital Sky Survey; cf. Lépine & Gaidos 2011). In collaboration with Sebastien Lépine, we observed and analysed an extension of the Lépine & Gaidos (2011) catalogue of high proper-motion candidates brighter than $J = 10.5$ mag. The spectra of stars brighter than $J = 9.0$ mag were published by Lépine et al. (2013), while most of the remaining fainter ones are published here.
- M dwarf candidates in nearby young moving groups (e.g., Montes et al. 2001; Zuckermann & Song 2004; da Silva et al. 2009; Shkolnik et al. 2012; Gagné et al. 2014; Klutsch et al. 2014), in multiple systems containing FGK-type primaries that are subjects of metallicity studies (Gliese & Jahreiss 1991; Poveda et al. 1994; Gould & Chanamé 2004; Rojas-Ayala et al. 2012; Terrien et al. 2012; Mann et al. 2013; Montes et al. 2013), in fragile binary systems at the point of disruption by the Galactic gravitational field (Caballero 2012, and references therein), and resulting from new massive virtual-observatory searches (Jiménez-Esteban et al. 2012; Aberasturi et al. 2014). Such a broad diversity of sources allowed us to widen the investigated intervals of age, activity, multiplicity, metallicity, and dynamical evolution.
- Known M dwarfs with well-determined spectral types from PMSU (see above) and Lépine et al. (2013). The comparison of these two samples with ours was a sanity check for determining the spectral types (see Sect. 4.1).
- M dwarfs in our input catalogue with uncertain or probably incorrect spectral types based on apparent magnitudes, $r' - J$ colours, and heliocentric distances, including resolved

[3] Please contribute to the comprehensiveness of our input catalogue by sending an e-mail with suggestions to José A. Caballero, e-mail: `caballero@cab.inta-csic.es`.

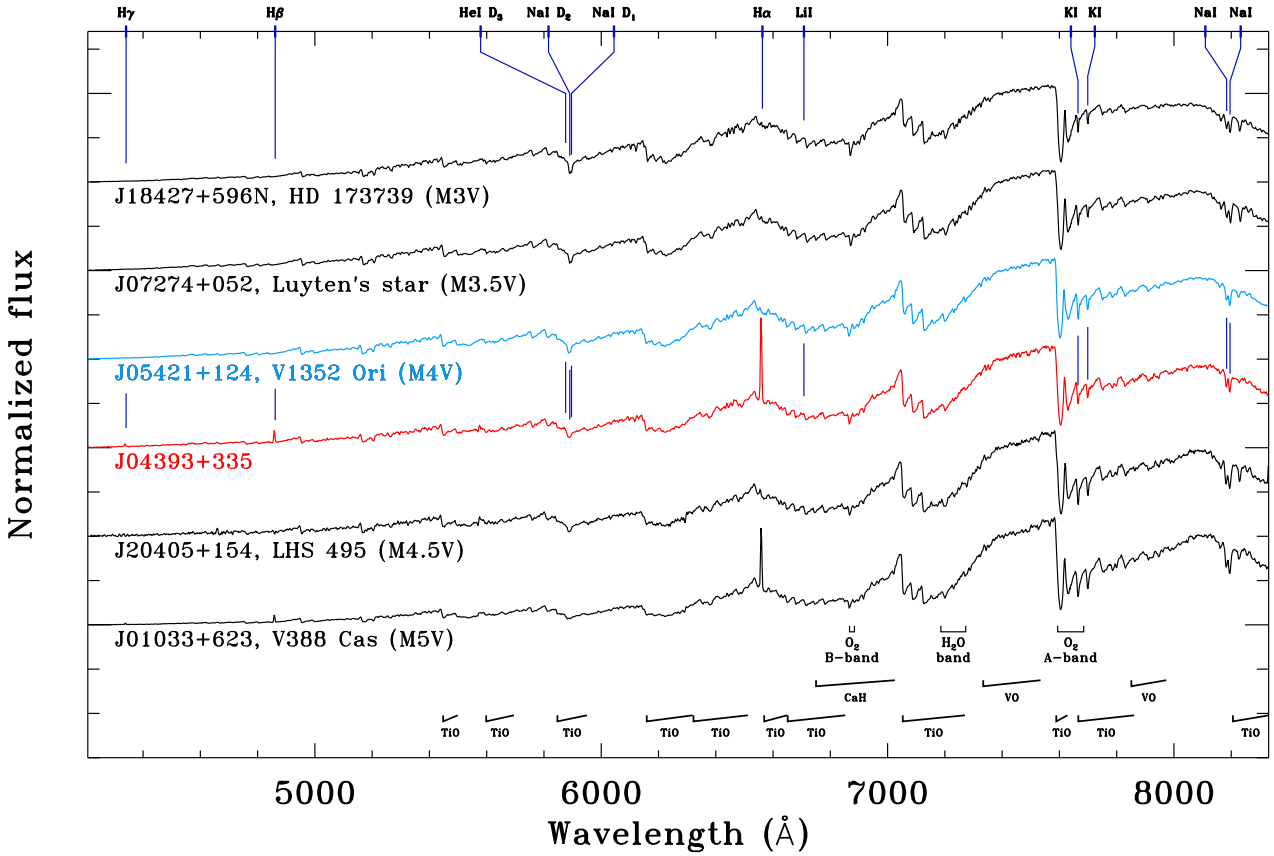

Fig. 1. Six representative CAFOS spectra. From top to bottom, spectra of standard stars with spectral type 1.0 and 0.5 subtypes earlier than the target (black), standard star with the same spectral type as the target (cyan), the target star (red; in this case, J04393+335 – M4.0 V, Simbad name: V583 Aur B), and standard stars with spectral type 0.5 and 1.0 subtypes later than the target (black). We mark activity-, gravity-, and youth-sensitive lines and doublets at the top of the figure (Hγ, Hβ, He I D$_3$, Na I D$_2$ and D$_1$, Hα, Li I, K I, and Na I, from left to right) and molecular absorption bands at the bottom. Note the three first lines of the Balmer series in emission in the spectrum of the target star.

physical binaries. See some examples in Cortés-Contreras et al. (2014).

– Numerous standard stars. For an accurate determination of spectral type and class, we also included approximately 50 stars with well-determined spectral types from K3 to M8 for both dwarf (Johnson & Morgan 1953; Kirkpatrick et al. 1991; PMSU) and giant classes (e.g., Moore & Paddock 1950; Ridgway et al. 1980; Jacoby et al. 1984; García 1989; Keenan & McNeil 1989; Kirkpatrick et al. 1991; Sánchez-Blázquez et al. 2006; Jiménez-Esteban et al. 2012).

3. Observations and analysis

3.1. Low-resolution spectroscopic data

Observations were secured with the Calar Alto Focal reductor and Spectrograph (CAFOS) mounted on the Ritchey-Chrétien focus of the Zeiss 2.2 m Calar Alto telescope (Meisenheimer 1994). We obtained more than 900 spectra of 745 targets during 38 nights over four semesters from 2011 November to 2013 April. All observations were carried out in service mode with the G-100 grism, which resulted in a useful wavelength coverage of 4200−8300 Å at a resolution $\mathcal{R} \sim 1500$. Exposure times ranged from shorter than 1 s to 1 h. The longest exposures were split into up to four sub-exposures. On some occasions, another star fell in the slit aperture (usually the primary of a close multiple system containing our M-dwarf candidate main target). We also added the 13 red dwarfs and giants observed in 2011 March by Jiménez-Esteban et al. (2012), which made a total of 758 targets.

We reduced the spectra using typical tasks within the IRAF environment. The reduction included bias subtraction, flat fielding, removal of sky background, optimal aperture extraction, wavelength calibration (with Hg-Cd-Ar, He, and Rb lamps), and instrumental response correction. For the latter, we repeatedly observed the spectrophotometric standards G 191–B2B (DA0.8), HD 84937 (sdF5), Feige 34 (sdO), BD+25 3941 (B1.5 V), and BD+28 421 (sdO) at different air masses. In the end, we only used the spectra with the highest signal-to-noise ratio of the hot subdwarf Feige 34, which gave the best-behaved instrumental response correction. We extracted all traces in the spectra, including those of other stars in the slit aperture. We did not remove telluric absorption lines from the spectra that were due to the variable meteorological conditions during two years of observation (see Sect. 3.2.2). All our spectra had a signal-to-noise ratio higher than 50 near the Hα λ6562.8 Å line, which together with the wide wavelength coverage allowed us to make a comprehensive analysis and to measure numerous spectral indices and activity indicators.

Table 3. Standard and prototype stars.

SpT		Karmn	Name
M0.0 V	*	J09143+526	HD 79210
		J07195+328	BD+33 1505
		J09144+526	HD 79211
M0.5 V	*	J18353+457	BD+45 2743
		J04329+001S	LP 595–023
		J22021+014	HD 209290
M1.0 V	*	J00183+440	GX And
		J05151–073	LHS 1747
		J11054+435	BD+44 2051A
M1.5 V	*	J05314–036	HD 36395
		J00136+806	G 242–048
		J01026+623	BD+61 195
		J11511+352	BD+36 2219
M2.0 V	*	J08161+013	GJ 2066
		J03162+581N	Ross 370 B
		J03162+581S	Ross 370 A
M2.5 V	*	J11421+267	Ross 905
		J10120–026 AB	LP 609–071
		J19169+051N	V1428 Aql
		J21019–063	Wolf 906
M3.0 V	*	J18427+596N	HD 173739
		J17364+683	BD+68 946
		J22524+099	σ Peg B
M3.5 V	*	J07274+052	Luyten's star
		J17199+265	V647 Her
		J17578+046	Barnard's star
		J18427+596S	HD 173740
M4.0 V	*	J05421+124	V1352 Ori
		J04308–088	Koenigstuhl 2 A
		J06246+234	Ross 64
		J10508+068	EE Leo
M4.5 V	*	J20405+154	G 144–025
		J04153–076	o^{02} Eri C
		J16528+610	GJ 625
		J17198+265	V639 Her
M5.0 V	*	J01033+623	V388 Cas
		J16042+235	LSPM J1604+2331
		J23419+441	HH And
M5.5 V	*	J02022+103	LP 469–067
		J21245+400	LSR J2124+4003
M6.0 V	*	J10564+070	CN Leo
		J07523+162	LP 423–031
		J16465+345	LP 276–022
M6.5 V	*	J08298+267	DX Cnc
		J09003+218	LP 368–128
		J10482–113	LP 731–058
M7.0 V	*	J16555-083	V1054 Oph D (vB 8)
		J02530+168	Teegarden's star
M8.0 V	*	J19169+051S	V1298 Aql (vB 10)

Notes. Prototype stars are marked with an asterisk.

We list in Table A.1 the 753 observed K and M dwarf and giant candidates according to identification number, our CARMENCITA identifier, discovery name, Gliese or Gliese & Jahreiß number, J2000.0 coordinates and J-band magnitude from the Two-Micron All-Sky Survey (Skrutskie et al. 2006), observation date, and exposure time. The five stars not tabulated are the spectrophotometric standards.

In Table A.1, our CARMENCITA identifier follows the nomenclature format "Karmn JHHMMm±DDd(X)", where "Karmn" is the acronym, "m" and "d" in the sequence are the truncated decimal parts of a minute or degree of the corresponding equatorial coordinates for the standard equinox of J2000.0 (IRAS style for right ascension, PKS quasar style for declination), and X is an optional letter (N, S, E, W) to distinguish between physical or visual pairs with the same HHMMm±DDd sequence within CARMENCITA. We use the discovery name for every target, except for M dwarfs with variable names (e.g., EZ PSc, GX And, V428 And) or those that are physical companions to bright stars (e.g., BD–00 109 B, η Cas B, HD 6440 B). We associate for the first time many X-ray events with active M dwarfs (e.g., Lalitha et al. 2012; Montes et al. 2015). In these cases, we use the precovery[4] *Einstein* 2E or *ROSAT* RX/1RXS event identifications instead of the names given by the proper-motion survey that recovered the stars.

Additionally, we always indicate whether the star is a known close binary or triple unresolved in our spectroscopic data (with "AB", "BC", "ABC"). There are 75 such close multiple systems in our sample (70 double and 5 triple), of which the widest unresolved pair is J09045+164 AB (BD+16 1895), with $\rho \approx 4.1$ arcsec. A comprehensive study on the multiplicity of M dwarfs in CARMENCITA, including spectral-type estimate of companions from magnitude differences in high-resolution imaging data, will appear in a forthcoming paper of this series (preliminary data were presented in Cortés-Contreras et al. 2015).

3.2. Spectral typing

We followed two widely used spectral classification schemes that require an accurate, wide grid of reference stars. The first strategy relies on least-squares minimisation and best-fitting to spectra of the standard stars, while the second scheme uses spectral indices that quantify the strength of the main spectral features in M dwarfs, notably molecular absorption bands (again, preliminary data were presented in Klutsch et al. 2012 – least-squares minimisation – and Alonso-Floriano et al. 2013a – spectral indices).

Before applying the two spectral-typing strategies, we normalised our spectra by dividing by the observed flux at 7400 Å. We also corrected for spatial distortions at the reddest wavelengths (with $R \sim 1500$, there is no need for a stellar radial-velocity correction). For that, we shifted our spectra until the K I $\lambda\lambda$7664.9, 7699.0 Å doublet was placed at the laboratory wavelengths. This correction, often of 1–2 Å, was critical for the definition of spectral indices, some of which are very narrow.

3.2.1. Spectral standard and prototype stars

We list the used standard stars in Table 3 (see also Sect. 3.2.4), most of which were taken from Kirkpatrick et al. (1991) and PMSU (Table 2). Our intention was to provide one prototype star and up to four reference stars per half subtype, but this was not always possible, especially at the latest spectral types. The prototype stars, shown in Fig. 2, are the brightest, least active reference stars that have spectra with the highest signal-to-noise ratio, and that do not deviate significantly from the general trend during fitting. In Table 3, the first star of each subtype is the prototype for that subtype. In the case of standard stars with different reported spectral types in the bibliography (with maximum

[4] "Pre-discovery recovery".

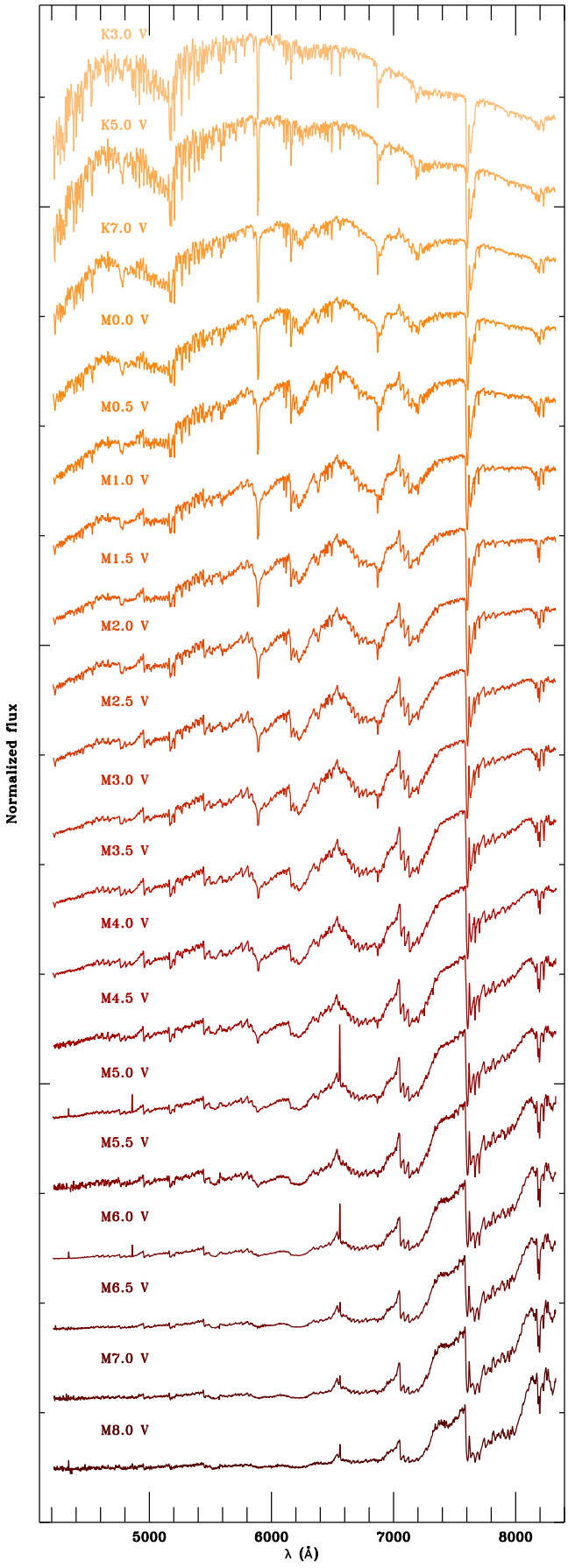

Fig. 2. CAFOS spectra of our prototype stars. From top to bottom, K3 V, K5 V, K7 V, M0.0–7.0 V in steps of 0.5 subtypes, and M8.0 V.

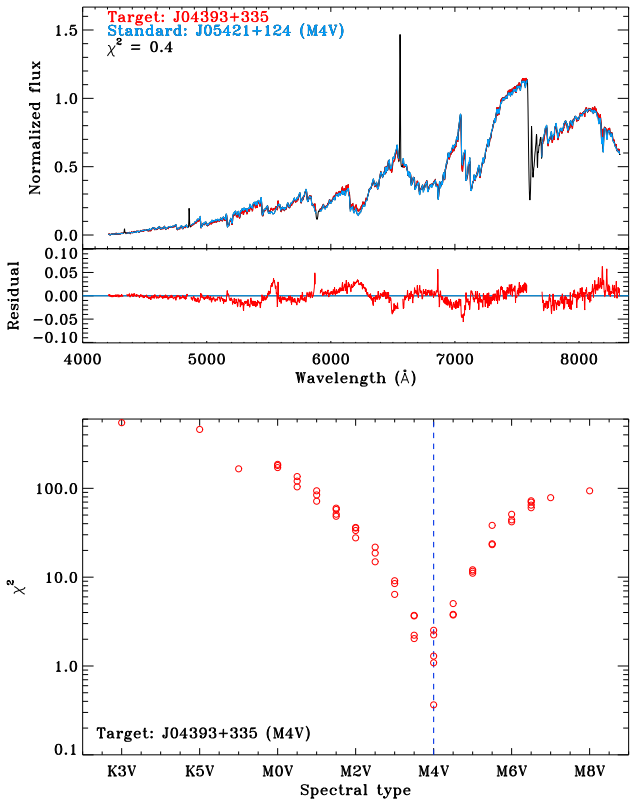

Fig. 3. Spectral typing of J04393+335 with best-match and $\chi^2_{\rm min}$ methods. *Top panel*: best-match. CAFOS normalised spectra of the target star and of the standard star that fits best (*top*) and the difference (*bottom*). *Bottom panel*: $\chi^2_{\rm min}$. Values of χ^2 as a function of the spectral type (open red circles). The vertical dashed line marks the spectral type at the lowest χ^2 value. Note the logarithmic scale in the Y axis.

differences of 0.5 subtypes), we chose the value that gave us less scatter in our fits.

We also used three K dwarfs from Kirkpatrick et al. (1991), not listed in Table 3, to extend our grid of standard stars towards warmer effective temperatures. The three K-dwarf standard stars are HD 50281 (K3 V), 61 Cyg A (K5 V), and η Cas B (K7 V). The standard star LP 609–071 AB is a close binary composed of an M2.5 V star and a faint companion separated by $\rho = 0.18 \pm 0.02$ arcsec (Delfosse et al. 1999). With $\Delta K = 0.95 \pm 0.05$ mag, the faint companion flux barely affects the primary spectrum in the optical.

3.2.2. Best-match and $\chi^2_{\rm min}$ methods

Before any least-squares minimisation, we discarded five narrow (20–30 Å) wavelength ranges influenced by activity indicators (Hα, Hβ, Hγ, and the Na I doublet – Fraunhofer C, F, and G′ lines) and by strong telluric lines (O_2 band around 7594 Å – Fraunhofer A line). Next, in the full remaining spectral range, we compared the normalised spectrum of every target star with those of all our standard stars in Table 3 and computed a χ^2 value for each fit. In the best-match method, we assigned the spectral type of the standard star that best fitted our target spectrum (i.e., with the lowest χ^2 value); in the $\chi^2_{\rm min}$ method, we assigned the spectral type that corresponded to the minimum of the curve resulting from the (sixth-order) polynomial fit of all the χ^2-spectral type pairs. As expected, the best-match and $\chi^2_{\rm min}$ methods give the same result in most cases. In the representative case shown

Table 4. Spectral indices used in this work.

Index	$\Delta\lambda_{num}$ [Å]	$\Delta\lambda_{den}$ [Å]	Reference
CaOH	6230:6240	6345:6354	Reid et al. (1995)
CaH 1	6380:6390	∑ 6345:6355, 6410:6420	Reid et al. (1995)
I2 (CaH)	6510:6540	6370:6400	Martín & Kun (1996)
I3 (TiO)	6510:6540	6660:6690	Martín & Kun (1996)
Hα	6560:6566	6545:6555	Reid et al. (1995)
TiO 1	6718:6723	6703:6708	Reid et al. (1995)
CaH 2	6814:6846	7042:7046	Reid et al. (1995)
CaH 3	6960:6990	7042:7046	Reid et al. (1995)
TiO-7053	7000:7040	7060:7100	Martín et al. (1999)
Ratio A (CaH)	7020:7050	6960:6990	Kirkpatrick et al. (1991)
TiO-7140	7015:7045	7125:7155	Wilking et al. (2005)
PC1	7030:7050	6525:6550	Martín et al. (1996)
CaH Narr	7044:7049	6972.5:6977.5	Shkolnik et al. (2009)
TiO 2	7058:7061	7043:7046	Reid et al. (1995)
TiO 3	7092:7097	7079:7084	Reid et al. (1995)
TiO 5	7126:7135	7042:7046	Reid et al. (1995)
TiO 4	7130:7135	7115:7120	Reid et al. (1995)
VO-a	∑ 7350:7370, 7550:7570	7430:7470	Kirkpatrick et al. (1999)
VO	∑ α7350:7400, β7510:7560[a]	7420:7470	Kirkpatrick et al. (1995)
Ratio B (Ti I)	7375:7385	7353:7363	Kirkpatrick et al. (1991)
VO-7434	7430:7470	7550:7570	Hawley et al. (2002)
PC2	7540:7580	7030:7050	Martín et al. (1996)
VO 1	7540:7580	7420:7460	Martín et al. (1999)
TiO 6	7550:7570	7745:7765	Lépine et al. (2003)
VO-b	∑ 7860:7880, 8080:8100	7960:8000	Kirkpatrick et al. (1999)
VO 2	7920:7960	8130:8150	Lépine et al. (2003)
VO-7912	7990:8030	7900:7940	Martín et al. (1999)
Ratio C (Na I)	8100:8130	8174:8204	Kirkpatrick et al. (1991)
Color-M	8105:8155	6510:6560	Lépine et al. (2003)
Na-8190	8140:8165	8173:8210	Hawley et al. (2002)
PC3	8235:8265	7540:7580	Martín et al. (1996)

Notes. [(a)] $\alpha = 0.5625, \beta = 0.4375$.

in Figs. 1 and 3, the target dwarf has an M4.0 V spectral type using both the best match and χ^2_{min} methods.

3.2.3. Spectral indices

The spectral indices methodology for spectral typing is based on computing flux ratios at certain wavelength intervals in low-resolution spectra (e.g., Kirkpatrick et al. 1991; Reid et al. 1994; Martín et al. 1996, 1999). In the present analysis, we compiled 31 spectral indices defined in the literature to determine spectral types of late-K dwarfs and M dwarfs that occur in the useable wavelength interval of our CAFOS spectra. In general, a spectral index I_i is defined by the ratio of numerator and denominator fluxes (i.e., $I_i = F_{i,num}/F_{i,den}$). Table 4 lists the 31 wavelength intervals of fluxes in the numerator and denominator, $\Delta\lambda_{num}$ and $\Delta\lambda_{den}$, and corresponding reference for each index. Some flux wavelength intervals are the linear combination of two subintervals (CaH 1, VO-a, VO-b) or, in the case of the VO index, a non-linear combination. Additionally, there are wavelength intervals of fluxes in the numerator that are either redder and bluer than the one in the denominator, which translates into different slopes in the index-spectral type relations. Of the 31 tabulated indices, nine are related to TiO features, seven to VO, six to CaH, three to the "pseudo-continuum" (i.e., relative absence of features), and the rest to H and neutral metallic lines (Ti, Na).

For every star observed with CAFOS, we computed the stellar numerator and denominator fluxes using an automatic trapezoidal integration procedure. When all indices were available, we plotted all spectral index vs. spectral type diagrams for the standard stars listed in Table 3 and fitted low-order polynomials to the data points. Although some spectral indices allowed linear (e.g., I2, Ratio B) or parabolic fits, most of the fits were to cubic polynomials of the form $\mathrm{SpT}(i) = a + b\,i + c\,i^2 + d\,i^3$, where i was the index. In all cases, we checked our diagrams and fits with those in the original papers and found no significant differences (of less than 0.5 subtypes). We also took special care in defining the range of application of our fits in spectral type. The different shapes of fitting curves, ranges of application, and internal dispersion of the data points are illustrated in Fig. 4.

Some indices are sensitive not only to spectral type (i.e., effective temperature), but also to surface gravity (e.g., I2, Ratio A, CaH Narr, Ratio C, Na-8190 – Sect. 4.2), metallicity (e.g., CaOH, CaH 1, CaH 2, CaH 3 – Sect. 4.3), or activity (Hα – Sect. 4.4). We identified the spectral indices with the widest range of application and least scatter. Table 5 lists the coefficients of the cubic polynomial fits of the five spectral indices that we eventually chose for spectral typing (note the logarithmic scale of the Color-M index). The spectral index vs. spectral type diagrams of VO-7912 and Color-M are very similar to those of PC, TiO 2, and TiO 5, shown in Fig. 4. All of them are valid from

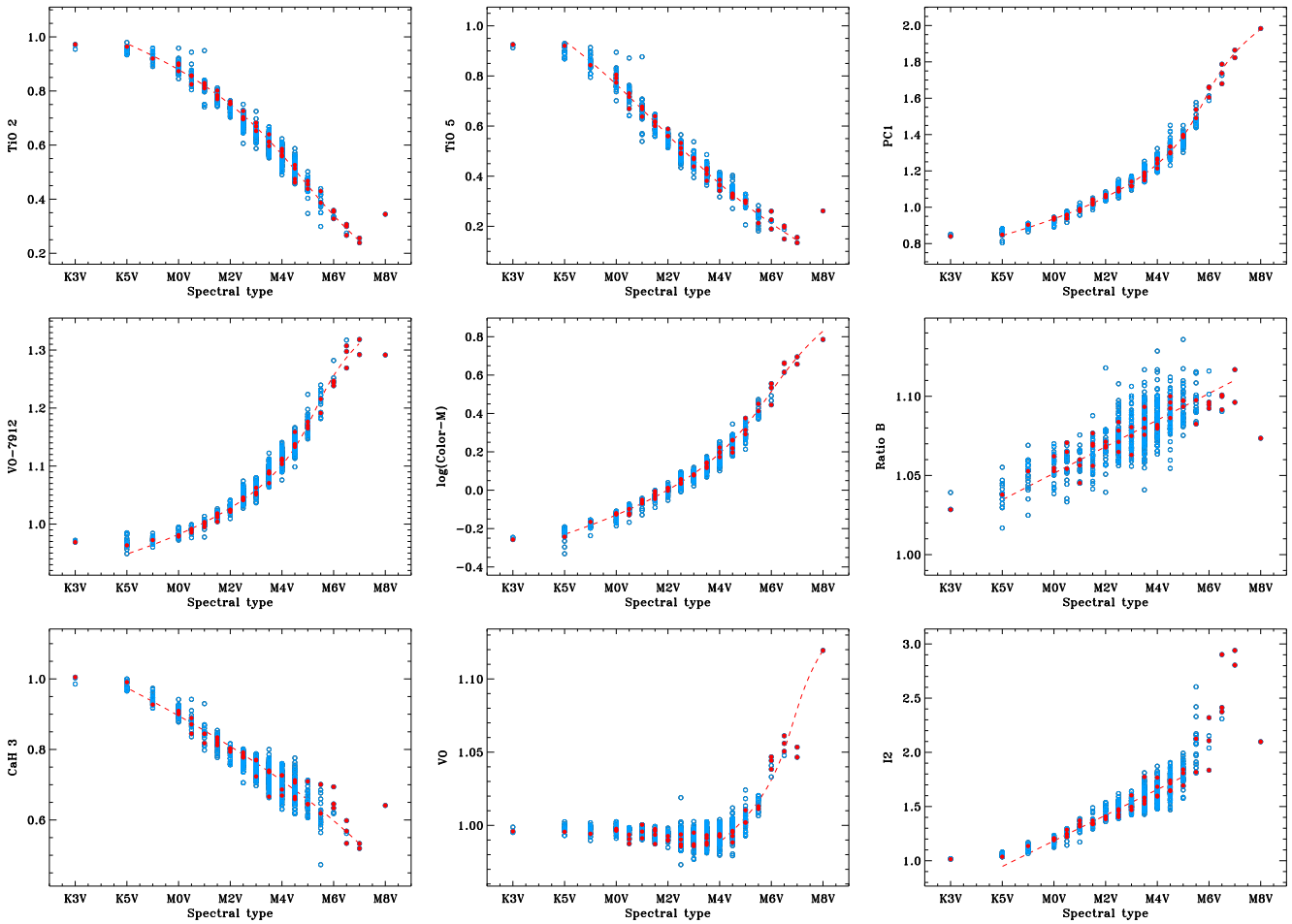

Fig. 4. Nine representative spectral indices as a function of spectral type. Filled (red) circles: standard stars. Open (blue) circles: remaining target stars. Dashed (red) line: fit to straight line, parabola, or cubic polynomial, drawn only in the range of application of the fit. *Top left and middle*: TiO 2 and TiO 5 (Reid et al. 1995), with negative slopes and useable up to M7 V; *top right*: PC1 (Martín et al. 1996), a monotonous spectral indicator from K5 V to M8 V; *centre left and middle*: VO-7912 (Martín et al. 1999) and Color-M (Lépine et al. 2003), two indices very similar to the PC1. Note the logarithmic scale in Color-M; *centre right*: ratio B (Kirkpatrick et al. 1991), sensitive to several stellar parameters and, thus, with a large scatter in the spectral type relation; *bottom left*: CaH 3 (Reid et al. 1995), with a slightly larger scatter than pseudo-continuum or titanium oxide indices, due to metallicity; *bottom middle*: VO (Kirkpatrick et al. 1995), useable only for determining spectral types later than M4 V; *bottom right*: I2 (Martín & Kun 1996), with a linear range of variation from mid-K to mid-M and a sudden increase (or high dispersion) at late-M.

K7 V to M7 V (to M8 V in the case of PC1 and Color-M), while the dispersion of the fits is of about 0.5 subtypes. The TiO 5 has been a widely used index for spectral typing (Reid et al. 1995; Gizis 1997; Seeliger et al. 2011; Lépine et al. 2013) but, to our knowledge, we propose here for the first time to use it with a nonlinear fit.

In Table A.2, we list the values of the five spectral-typing indices of all CAFOS stars together with the CaH 2 and CaH 3 indices that are used to compute the ζ metallicity index (Sect. 4.3) and the pseudo-equivalent width of the Hα line (Sect. 4.4).

3.2.4. Adopted spectral types

After applying the best-match and $\chi^2_{\rm min}$ methods and using the five spectral-index-type relations in Table 5, we obtained seven complementary spectral-type determinations for each star. In Table A.3, we assigned a value between 0.0 and 8.0 in steps of 0.5 to each M spectral subtype for all stars of dwarf luminosity class (there are no stars later than M8.0 V in our CAFOS sample). In addition, we used the values –2.0 and –1.0 for referring to K5 V and K7 V spectral types (there are no K6, 8, 9 spectral types in the standard K-dwarf classification – Johnson & Morgan 1953; Keenan & McNeil 1989). In some cases, we were able to identify dwarfs earlier than K5 V with the best-match and $\chi^2_{\rm min}$ methods. For giant stars, we only provide a visual estimation

Table 5. Coefficients and standard deviation (in spectral subtypes) of the cubic polynomial fits of the five spectral-typing indices.

Index	a	b	c	d	σ
TiO 2	+11.0	–22	+28	–20	0.83
TiO 5	+9.6	–20	+17.0	–9.0	0.57
PC1	–50	+97	–59	+12.4	0.52
VO-7912	–520	+1300	–1070	+300	0.59
Color-M	+1.98	+13.1	–15.6	+10.3	0.53

Notes. We used the relation SpT(i) = $a + b\,i + c\,i^2 + d\,i^3$ for the cubic fits. For the Color-M index we used the relation SpT(i) = $a + b\,\log i + c\,(\log i)^2 + d\,(\log i)^3$.

(K III, M III) based on the spectral types of well-known giant standard stars observed with CAFOS.

For all late-K and M dwarfs, we calculated one single spectral type per star based on the information provided by the seven individually determined spectral indices. We used a median of the seven values for cases where they were identical within 0.5 subtypes. To avoid any bias, we carefully checked the original spectra if the spectral types from the best-match and $\chi^2_{\rm min}$ methods and from the spectral indices were different by 0.5 subtypes, or if any spectral type deviated by 1.0 subtypes or more (which occurred very rarely). In these cases, we adopted the spectral type of the closest (visually and in χ^2) standard star. The uncertainty of the adopted spectral types is 0.5 subtype, except for some odd spectra indicated with a colon (probably young dwarfs of low gravity or subdwarfs of low metallicity; see below).

4. Results and discussion

4.1. Spectral types

Among the 753 investigated stars with adopted spectral types from CAFOS data, there were 23 late-K dwarfs at the K/M boundary (K7 V), 21 early- and intermediate-K dwarfs (K0−5 V), 22 M-type giants (M III), three K-type giants (K III), and one star without class determination (i.e., J04313+241 AB). This left 683 M-type dwarfs (and subdwarfs) in our CAFOS sample.

As shown in Table A.3, we searched for previous spectral type determinations in the literature for the 753 investigated stars (small "m" and "k" denote spectral types estimated from photometry). Taking previous determinations and estimations into account, we derived spectral types from spectra for the first time for 305 stars, and revised typing for most of the remaining 448 stars.

The agreement in spectral typing with previous large spectroscopic surveys of M dwarfs is shown in Fig. 5. The standard deviations of the differences between the spectral types derived by us and by PMSU (with a narrower wavelength interval; 100 stars in common) and by Lépine et al. (2013; 95 stars in common) were 0.55 and 0.38 subtypes, respectively, which are of the order of our internal uncertainty (0.5 subtypes). The standard deviation of the differences between our spectral types and those estimated from photometry by Lépine & Gaidos (2011; 576 stars in common) is larger, of up to 1.32 subtypes. The bias towards later spectral types in Lépine & Gaidos (2011) and the scatter of the spectral type differences is obvious from the bottom panel in Fig. 5. In particular, we measured maximum differences of up to 7 subtypes, by which some late-M dwarf candidates become actual K dwarfs (probably due to the use by Lépine & Gaidos of B_J and R_F from photographic plates for the spectral type estimation; see references in Sect. 2). However, over 93% of the compared stars have disagreements lower than or equal to 2 subtypes. We emphasize that our CARMENCITA data base is very homogeneous because more than 95% of the spectral type determinations come from either PMSU, Lépine et al. (2013), or our CAFOS data, which are consistent with each other, as shown above.

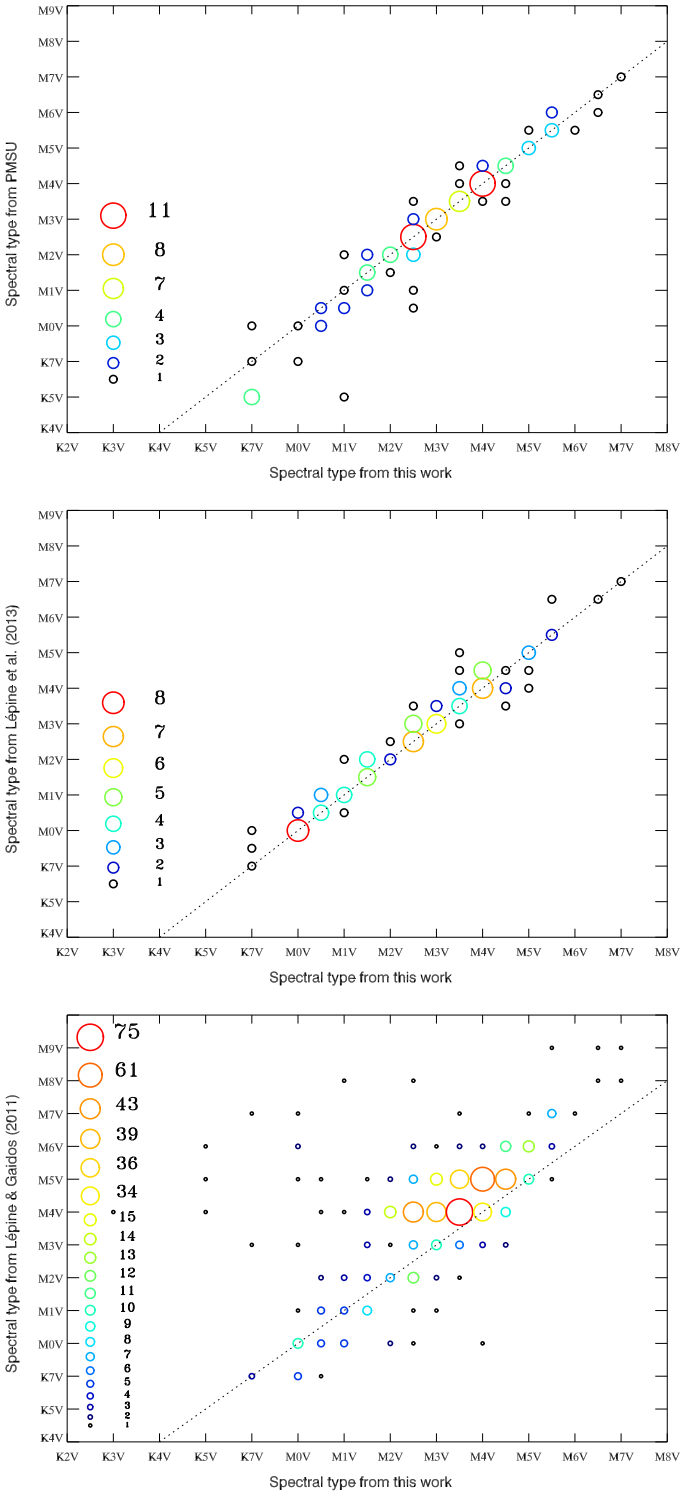

Fig. 5. Spectral type comparison between our results and those from PMSU (*top panel*), Lépine et al. (2013; *middle panel*), and Lépine & Gaidos (2011; from $V^* - J$ photometry, *bottom panel*). The larger a circle, the greater the number of stars on a data point. Dotted lines indicate the one-to-one relationship.

Of the 683 CAFOS M-type dwarfs (and subdwarfs), 414 and 106 M dwarfs satisfy our criteria in Table 1 of restrictive J-band spectral type limiting and completeness, respectively. In total, 261 dwarfs have spectral type M4.0 V or later. The brightest, latest of them are being followed-up with high-resolution spectrographs and imagers and with data from the bibliography to identify the most suitable targets for CARMENES (no physical or visual companions at less than 5 arcsec, low $v \sin i$; see forthcoming papers of this series). Furthermore, there are 61 relatively bright ($J < 10.9$ mag) CAFOS stars with spectral types

Table 6. Giant stars observed with CAFOS.

Karmn	Name	Giant
J00146+202	χ Peg	Standard
J00367+444	V428 And	Standard
J00502+601	HD 236547	Standard
J01012+571	1RXS J010112.8+570839	New
J01097+356	Mirach	Standard
J02479–124	Z Eri	Standard
J02558+183	ρ^{02} Ari	Standard
J03319+492	TYC 3320–337–1	LG11[a]
J04206–168	DG Eri	Standard
J07420+142	NZ Gem	Standard
J10560+061	56 Leo	Standard
J11018–024	p^{02} Leo	Standard
J11201+301	HD 98500	Standard
J11458+065	ν Vir	Standard
J12322+454	BW CVn	Standard
J12456+271	HD 110964	Standard
J12533+466	BZ CVn	Standard
J13587+465	HD 122132	Standard
J17126–099	Ruber 7	JE12[b]
J17216–171	TYC 6238–480–1	JE12[b]
J18423–013	Ruber 8	JE12[b]
J22386+567	V416 Lac	Standard
J23070+094	55 Peg	Standard
J23177+490	8 And	Standard
J23266+453	2MASS J23263798+4521054	Background

References. [(a)] LG11: Lépine & Gaidos (2011). [(b)] JE12: Jiménez-Esteban et al. (2012).

between M5.0 V and M8.0 V that are also suitable targets for any other near-infrared radial-velocity monitoring programmes with the instruments mentioned above (i.e., HPF, SPIRou, IRD).

4.2. Gravity

Table 6 lists the 25 giants observed with CAFOS. Of these, 17 stars have previously been tabulated as M giant standard stars (e.g., Keenan & McNeil 1989; García 1989; Kirkpatrick et al. 1991; Sánchez-Blázquez et al. 2006). They are bright ($J \lesssim 5.0$ mag; down to -1.0 mag in the case of Mirach, β And) and show the low-gravity spectral features typically found in M giants: faint alkali lines (K I $\lambda\lambda$7665, 7699 Å and Na I $\lambda\lambda$8183, 8195 Å), a tooth-shaped feature produced by MgH/TiO blend near 4770 Å, and a decrease of CaH in the A-band at 6908–6946 Å with the increase of luminosity (Kirkpatrick et al. 1991; Martín et al. 1999; Riddick et al. 2007; Gray & Corbally 2009). Two other stars, V428 And and HD 236547, are well-known K giant standard stars (Jacoby et al. 1984; García 1989; Kirkpatrick et al. 1991).

Of the other six giant stars in Table 6, three have J-band magnitudes of 6.1−6.2 mag and were identified by Jiménez-Esteban et al. (2012) as some of the reddest Tycho-2 stars with proper motions $\mu > 50$ mas a^{-1}, namely Ruber 7, TYC 6238–480–1, and Ruber 8 (which seems to be also one of the brightest metal-poor M giants ever identified). The remaining three giant stars, with faint J-band magnitudes between 8.2 and 10.0 mag, are listed below.

– J01012+571 (1RXS J010112.8+570839). It is a previously unknown distant M giant close to the Galactic plane ($b = -5.7$ deg). It was serendipitously identified in an unpublished photometric survey by one of us (J.A.C.), and was observed with CAFOS because of its very red optical and near-infrared colours and possible association with an X-ray event catalogued by *ROSAT* at a separation of only 6.4 arcsec.
– J03319+492 (TYC 3320–337–1). From photographic magnitudes, Pickles & Depagne (2010) and Lépine & Gaidos (2011) classified it as an M1.9 and M3 dwarf, respectively. However, it appears to be an early-K giant with a significant proper motion of 56 mas a^{-1}. It is not possible to separate it from the main sequence in a reduced proper-motion diagram.
– J23266+453 (2MASS J23263798+4521054). Our intention was to observe BD+44 4419 B (G 216–43), an M4.5 dwarf of roughly the same V-band magnitude (10.3 vs. 10.9 mag). Unfortunately, we incorrectly observed instead a background giant at a separation of about 20 arcsec.

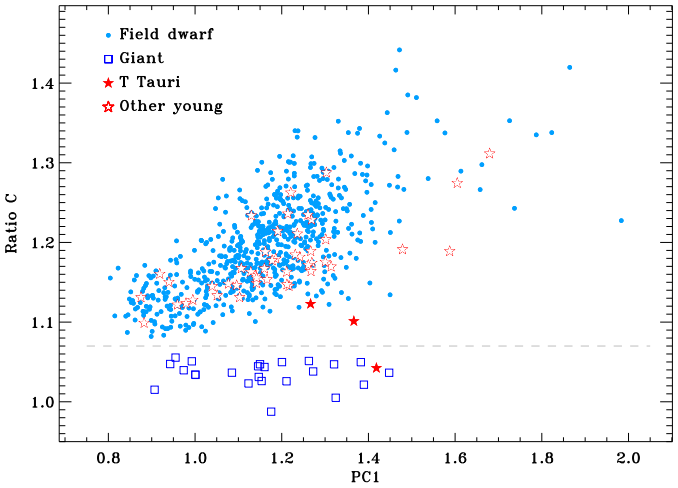

Fig. 6. Ratio C vs. PC1 index-index diagram. The different symbols represent field dwarfs (small dots, blue), giants (open squares, dark blue), Taurus stars (filled stars, red), and other young stars (open stars, red). All giants are below the dashed line at Ratio C = 1.07. The dashed line is the empirical border of the giant star region.

In a Ratio C vs. PC1 index-index diagram as the one shown in Fig. 6, where Ratio C is highly sensitive to gravity and PC1 is an effective temperature proxy (PC1 was indeed one of the five indices used for deriving spectral types), all giants are below the dashed line at Ratio C = 1.07. There is only one star not classified as a giant that lies below that empirical boundary. It is J04313+241 (V927 Tau AB), a T Tauri star for which we did not provide a luminosity class in Sect. 4.1. We discuss this in detail in Sect. 4.4. Ratio C, which contains the sodium doublet at 8193, 8195 Å, can also be used as a youth indicator (e.g., Schlieder et al. 2012b).

4.3. Metallicity

In F-, G-, and K-type stars whose photospheric continua are well-defined in high-resolution spectra, stellar metallicity is computed through spectral synthesis (McWilliam 1990; Valenti & Piskunov 1996; González 1997; González Hernández et al. 2004; Valenti & Fischer 2005; Recio-Blanco et al. 2006) or measuring equivalent widths, especially of iron lines (Sousa et al. 2008, 2011; Magrini et al. 2010; Adibekyan et al. 2012; Tabernero et al. 2012; Bensby et al. 2014). However, it is

not possible to measure a photospheric continuum in M-type stars and, thus, their metallicity is studied through other techniques. Since the first determinations from broad-band photometry by Stauffer & Hartmann (1986), there have been three main observational techniques employed to determine metallicity in M dwarfs:

- Photometry calibrated with M dwarfs in physical double and multiple systems with warmer companions, typically F, G, K dwarfs, of known metallicity (Bonfils et al. 2005; Casagrande et al. 2008; Schlaufman & Laughlin 2010; Neves et al. 2012).
- Low-resolution spectroscopy, also calibrated with M dwarfs with earlier primaries, in the optical (Dhital et al. 2012), in the near infrared (Rojas-Ayala et al. 2010, 2012; Terrien et al. 2012; Mann et al. 2014; Newton et al. 2014), or in both wavelength ranges (Mann et al. 2013, 2015).
- High-resolution spectroscopy in the optical (from spectral synthesis: Woolf & Wallerstein 2005; from spectral indices: Woolf & Wallerstein 2006; and Bean et al. 2006; from the measurement of pseudo-equivalent widths: Neves et al. 2013, 2014), in the near-infrared (Shulyak et al. 2011, in the *Y* band; Önehag et al. 2012, in the *J* band; Tsuji & Nakajima 2014, in the *K* band), or in the optical and near-infrared simultaneously (Gaidos & Mann 2014). The novel mid-resolution spectroscopy study in the optical aided with spectral synthesis by Zboril & Byrne (1998) also belongs in this item.

For the 753 CAFOS stars, we computed the $\zeta_{\rm TiO/CaH}$ metallicity parameter (denoted ζ for short) described by Lépine et al. (2007):

$$\zeta = \frac{1 - {\rm TiO\,5}}{1 - [{\rm TiO\,5}]_{Z_\odot}}, \quad (1)$$

where $[{\rm TiO\,5}]_{Z_\odot} = 0.571 - 1.697{\rm CaH} + 1.841{\rm CaH}^2 - 0.454{\rm CaH}^3$ is a third-order fit of CaH = CaH 2 + CaH 3 for *our* standard stars, and TiO 5, CaH 2, and CaH 3 are the spectral indices of Reid et al. (1995) (see also Gizis & Reid 1997; and Lépine et al. 2003). The ζ index is correlated with metallicity in metal-poor M subdwarfs (Woolf et al. 2009) and metal-rich dwarfs (Lépine et al. 2007; Mann et al. 2014). For completeness, we also tabulate the ζ index for our 25 giants, but they are not useful for a comparison. We made the same assumption of standard stars having solar metallicity ($\zeta \approx 1$) as in Lépine et al. (2007), which was later justified by the small dispersion of the data points.

We looked for M dwarfs (and subdwarfs) in our sample with abnormal metallicity, which could be spotted in a CaH 2 + CaH 3 vs. TIO 5 index-index diagram as in Fig. 7. Lépine et al. (2007) defined the classes subdwarf (sd), $0.5 < \zeta < 0.825$, and extreme subdwarf (esd), $\zeta < 0.5$. All our non-giant stars except two have ζ values greater than 0.825, which is the empirical boundary between dwarfs and subdwarfs. The spectra of the two exceptions show shallower molecular bands and lines than M dwarfs of the same spectral type.

One of our two subdwarf candidates is J19346+045 (sdM1:, $\zeta = 0.775$ – HD 184489). Some authors have reported features of low metallicity (e.g., Maldonado et al. 2010), but none had classified it as a subdwarf (but see Sandage & Kowal 1986). Its low effective temperature has prevented spectral synthesis analyses on high-resolution spectra.

The other new subdwarf candidate is J16354–039 (sdM0:, $\zeta = 0.664$ – HD 149414 B, BD–03 3968B). Giclas et al. (1959) discovered it and associated it with the G5 Ve single-line spectroscopic binary HD 149414 Aa,Ab. Afterwards, its membership in the very wide system has been investigated by Poveda et al. (1994), Tokovinin (2008), and Dhital et al. (2010), for example, and confirmed and quantified by Caballero (2009). The projected physical separation between Aa,Ab and B amounts to 53 000 au (about a quarter of a parsec). Remarkably, the primary is a halo binary of low metallicity ([Fe/H] ~ –1.4 – Strom & Strom 1967; Sandage 1969; Cayrel de Strobel et al. 1997; Holmberg et al. 2009). This explains the low ζ metallicity index of J16354–039 for its spectral type and the wide separation of the system (due to gravitational disruption by the Galactic gravitational potential or to common origin and ejection from the same cluster; cf. Caballero 2009, and references therein).

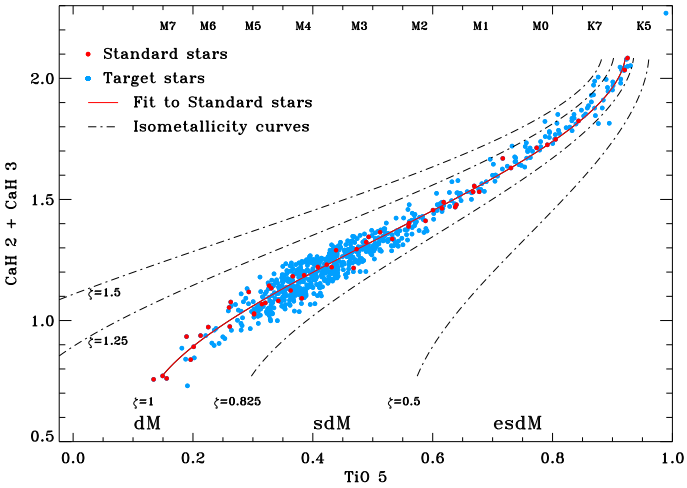

Fig. 7. CaH 2 + CaH 3 vs. TIO 5 index-index diagram of our CAFOS stars, after discarding giants. The spectral types at the top are indicative, but follow the TiO 5 fit given in Table 5. The solid and dash-dotted lines are iso-metallicity curves of the ζ index.

In addition, J12025+084 (M1.5 V; $\zeta = 0.898$ – LHS 320) was classified by Gizis (1997) as an sdM2.0 star and was investigated extensively afterwards with high-resolution imagers (Gizis & Reid 2000; Riaz et al. 2008; Jao et al 2009; Lodieu et al. 2009). However, we failed to detect any subdwarf signpost in our high signal-to-noise spectrum, which is partly consistent with the metallicity [Fe/H] = −0.6±0.3 measured by Rajpurohit et al. (2014).

No CAFOS star showed a very high metallicity index greater than $\zeta = 1.5$. In spite of the dispersion of the ζ index around unity, we considered that all our 726 dwarfs (753 stars in total minus the 25 giants and the two subdwarfs) *approximately* have solar metallicity ([Fe/H] ≈ 0.0). This assumption is relevant for instance to derive the mass from absolute magnitudes, the spectral types, and theoretical models that need metallicity as an input.

4.4. Activity

Chromospheric activity is one of the main relevant parameters for exoplanet detection around M dwarfs. The heterogeneities on the stellar surface of the almost-fully convective, rotating, M dwarfs, such as dark spots, may induce spurious radial-velocity variations at visible wavelengths

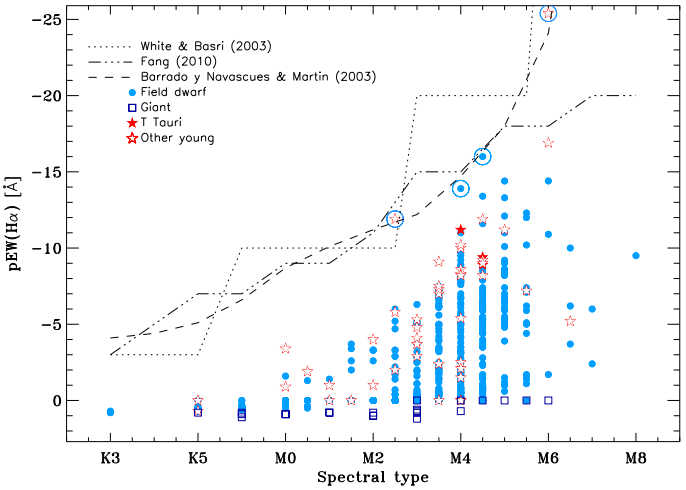

Fig. 8. Pseudo-equivalent width of Hα line vs. spectral type diagram. Measurement errors are 0.5 subtypes for the spectral type and are of the order of 10% with a minimum of 0.1 Å for pEW(Hα) (but scatter due to variability is probably larger than 10%). Dotted, dash-dotted, and dashed lines indicate the boundaries between chromospheric and accretion emission for different authors. Giants, plotted with open squares, have filled Hα lines or in absorption. None of the young stars, plotted with open and filled stars, show accretion emission. The four stars at the accretion boundary discussed in the text are encircled.

(Bonfils et al. 2007; Reiners et al. 2010; Barnes et al. 2011; Andersen & Korhonen 2015; Robertson et al. 2015). Near-infrared observations are expected to improve the precision of radial-velocity measurements with respect to the visible for stars cooler than M3, and CARMENES will cover the wavelength range from 0.55 to 1.70 μm. In spite of this, we plan to identify the least active stars for our exoplanet search. Moreover, several authors have identified significant differences between colours and spectral indices of active and inactive stars of similar properties that may affect the spectral typing of M dwarfs (Stauffer & Hartmann 1986; Hawley et al. 1996; Bochanski et al. 2007; Morales et al. 2008).

4.4.1. Hα emission

The Hα index (Reid et al. 1995) was one of the 31 indices measured on our CAFOS spectra (Table 4). For a better reliability on the activity determination and comparison with other works, we also measured the pseudo-equivalent width of the Hα line, pEW(Hα), of all the CAFOS stars (Table A.2). We here used pEW(Hα) as the proxy for activity (we used the pseudo-equivalent width of the line measured with respect to a local pseudo-continuum instead of the equivalent width because in M – and L, T, and Y – dwarfs the spectral continuum is not observable – e.g. Tsuji & Nakajima 2014).

We plot in Fig. 8 the pEW(Hα) vs. spectral type diagram for the whole sample. M dwarfs with late spectral types tend to show the Hα line in (strong) emission more often than earlier stars (see e.g. Hawley et al. 1996; West et al. 2004; or Reiners et al. 2013). There is a significant number of M4.0 V stars and later, however, that show very low Hα emission below 5 Å (in absolute values).

A few stars stand out in the pEW(Hα) vs. spectral type diagram in Fig. 8. Four of them lie at the boundary between chromospheric and accretion emission, as defined by Barrado y Navascués & Martín (2003), White & Basri (2003), and Fang (2010). Their high activity led us to investigate them in detail.

- J04290+186 (M2.5 V, pEW(Hα) = $-11.9^{+0.5}_{-0.3}$ Å, V1103 Tau). It is a member of the 600 Ma-old Hyades cluster (Johnson et al. 1962; Griffin et al. 1988; Stauffer et al. 1991; Reid 1992).
- J04544+650 (M4.0 V, pEW(Hα) = $-13.9^{+0.8}_{-0.5}$ Å, 1RXS J045430.9+650451). It is an anonymous Tycho-2 star (TYC 4087–1172–1; Lépine & Gaidos 2011) that we cross-matched with an aperiodic, variable, X-ray source identified by Fuhrmeister & Schmitt (2003). This X-ray variability and the presence of He I λ5875.6 Å in emission indicates that J04544+650 was flaring during our observations.
- J01567+305 (M4.5 V, pEW(Hα) = −16.0 ± 0.4 Å, NLTT 6496, Koenigstuhl 4 A). It forms a loosely bound common-proper-motion pair together with the M6.5: V star NLTT 6491 (Koenigstuhl 4 B), and is associated with an X-ray source (Caballero 2012). Interestingly, Aberasturi et al. (2014) collected low-resolution spectroscopy for J01567+305 just two months earlier, for which they determined a spectral type identical to ours within the uncertainties, but measured pEW(Hα) = −9.3 ± 0.3 Å, which is significantly lower than our measurement. Our CAFOS spectrum also shows He I in emission, so the mid-M dwarf likely underwent a flare during our observations.
- J07523+162 (M6.0 V, pEW(Hα) = $-25.4^{+1.4}_{-1.0}$ Å, LP 423−031). It has also been classified as a single M7 Ve star from optical spectra (Cruz et al. 2003; Reid et al. 2003; Gatewood & Coban 2009; Reiners & Basri 2009), but as an M6 V with surface gravity consistent with normal field dwarfs from near-infrared spectra (Allers & Liu 2013). From high-resolution spectroscopy (pEW(Hα) = −22.3 Å) and *ROSAT* X-ray count rates, Shkolnik et al. (2009) assigned J07523+162 an age of about 100 Ma, younger than the Pleiades. However, Reiners & Basri (2010) observed flaring activity in a J07523+162 spectrum (pEW(Hα) = −44.4 Å) and Gagné et al. (2014) and Klutsch et al. (2014) were not able to determine membership in any known stellar kinematic group.

There is an additional fifth active dwarf that stands out among the remaining stars in Fig. 8. It is J03332+462 (M0.0 V, pEW(Hα) = $-3.4^{+0.5}_{-0.3}$ Å, V577 Per B), a confirmed member of the ∼70 Ma-old AB Doradus moving group (Zuckerman et al. 2004; da Silva et al. 2009; Schlieder et al. 2012a). Its relatively bright primary at about 9 arcsec is a young K2 V star with strong ultraviolet and X-ray emission and lithium in absorption (Pounds et al. 1993; Jeffries 1995; Montes et al. 2001; Zuckerman & Song 2004; Xing & Xing 2012).

4.4.2. Young (and very young) stars

The identification of one open cluster member, one moving group member, and one purported young star in the field among five M dwarfs led us to examine the bibliography for other young star candidates in our CAFOS sample. The result of this bibliographic search is summarised in Table 7. In total, 49 spectroscopically investigated stars in this work have been reported to belong to the Taurus-Auriga star-forming region (∼1−10 Ma, three stars), β Pictoris moving group (∼12−22 Ma, five stars), Carina or Columba associations (∼15−50 Ma, two stars), Argus

Table 7. Reported young stars in our sample.

Karmn	Moving group/ association/cluster/ star-forming region	Ref.
J03332+462	AB Dor MG	See text
J03466+243 AB	Pleiades	vMa45
J03473–019	AB Dor MG	Zuc04
J03548+163 AB	Hyades	Gic62
J04123+162 AB	Hyades	Gic62
J04177+136 AB	Hyades	Gic62
J04206+272	Taurus	Sce07
J04207+152 AB	Hyades	Gic62
J04227+205	Hyades	Reid93
J04238+149 AB	Hyades	Gic62
J04238+092 AB	Hyades	Gic62
J04252+172 ABC	Hyades	Gic62
J04290+186	Hyades	Gic62
J04313+241 AB	Taurus	HR72
J04360+188	Hyades	Pels75
J04366+186	Hyades	See text
J04373+193	Hyades	Reid93
J04393+335	Taurus	Wic96
J04425+204 AB	Hyades	Reid93
J04430+187 AB	Hyades	Gic62
J05019+011	β Pic MG	Sch12
J05062+046	β Pic MG	Sch12
J05256–091 AB	AB Dor MG	Shk12
J05320–030	β Pic MG	daS09
J05415+534	Her-Lyr MG?	Eis13
J05457–223	UMa MG	Tab15
J06075+472	AB Dor MG	Sch12
J06246+234	Young	Mon01
J07319+362N	Castor MG	Cab10
J07319+362S AB	Castor MG	Cab10
J07361–031	Castor MG	Cab10
J07523+162	Young	See text
J08298+267	Castor MG	Cab10
J09328+269	Her-Lyr MG	Eis13
J09362+375	Young	Malo14
J10196+198 AB	Castor MG	Cab10
J10359+288	β Pic MG	Sch12
J10508+068	Her-Lyr MG?	Eis13
J11046–042S AB	Her-Lyr MG	Eis13
J13143+133 AB	Young	Sch14
J15079+762	IC 2391 MG	Mon01
J17198+265	Hyades SC	Klu14
J17199+265	Hyades SC	Klu14
J18313+649	AB Dor	Sch12
J21376+016	β Pic MG	Sch12
J22160+546	Her-Lyr MG?	Eis13
J22234+324 AB	AB Dor MG	Malo14
J23194+790	Carina/Columba Ass.	Klu
J23209–017 AB	Argus Ass.	Malo14
J23228+787	Carina/Columba Ass.	Klu

References. vMa45: van Maanen (1945); Gic62: Giclas et al. (1962); HR72: Herbig & Rao (1972); Pels75: Pels et al. (1975); Reid93: Reid (1993); Wic96: Wichmann et al. (1996); Mon01: Montes et al. (2001); Zuc04: Zuckerman et al. (2004); Sce07: Scelsi et al. (2007); daS09: da Silva et al. (2009); Cab10: Caballero (2010); Sch12: Schlieder et al. (2012a); Shk12: Shkolnik et al. (2012); Eis13: Eisenbeiss et al. (2013); Klu14: Klutsch et al. (2014); Malo14: Malo et al. (2014); Sch14: Schlieder et al. (2014); Tab15: Tabernero et al. (2015); Klu: Klutsch, priv. comm. Part of the content of this table was extracted from Hidalgo (2014).

association (~40 Ma, one star), AB Doradus moving group (~70−120 Ma, five stars), Pleiades cluster (~120 Ma, one star − with a relatively early K5 V spectral type), IC 2391 supercluster (~100−200 Ma, one star), Hercules-Lyra moving group (~200−300 Ma, four stars − note the question marks), Castor moving group (~200−300 Ma, six stars), Ursa Major moving group (~300−500 Ma, one star), and Hyades cluster and supercluster (~600 Ma, 14 and 2 stars, respectively), and four to the young ($\tau \lesssim 600$ Ma) field star population in the solar neighbourhood. See Zuckerman & Song (2004) and Torres et al. (2008) for reviews on young moving groups.

The actual existence of some of the entities above (e.g., Hercules-Lyra and Castor moving groups, and IC 2391 and Hyades superclusters) is questioned by several authors. Three of the five stars with the lowest Hα emission for their spectral type belong to the hypothetical Castor moving group (Barrado y Navascués 1998; Montes et al. 2001; Ribas 2003; Caballero 2010; Mamajek 2013; Zuckerman et al. 2013), and the other two to the Hyades (super-) cluster (van Altena 1966; Hanson 1975; Legget & Hawkins 1988; Hawley et al. 1996; Stauffer et al. 1997; Montes et al. 2001; Klutsch et al. 2014). However, the extreme youth of some targets is confirmed by detection of lithium in absorption, X-ray in emission, and common proper-motion to bona fide primaries in nearby young moving groups.

Eleven of the 16 Hyads are known to be binaries. The relatively large number and (apparent) high binary frequency is a natural consequence of the Malmquist bias, which leads to the preferential detection of intrinsically bright objects. Equal-mass binaries are brighter than single stars of the same spectral type (by up to 0.75 mag) and, thus, the frequency of binarity in our magnitude-limited sample is higher than in a bias-free, volume-limited sample. While most of our targets lie at 20−30 pc (Cortés-Contreras et al. 2015), the overbrightness of binary Hyads makes them to look as if they were located roughly at 30 pc instead at the nominal distance of the Hyades at about 46 pc. We suggest to investigate the actual multiplicity status of the five remaining *single* M dwarfs with a mid-resolution spectroscopic monitoring.

At $d \sim 140$ pc, the three Taurus stars in Table 7 are *not* in the solar neighbourhood. Since they are still on the Hayashi track of contraction, their radii are larger than those of dwarfs of the same effective temperature. As a result, they are also much more luminous, which explains why we were able to observe them even though they are located an order of magnitude farther away than the rest of our dwarf targets. As expected from their extreme youth, the three T Tauri stars have Hα emissions in the highest quartile (pEW(Hα)s between –9 and –11 Å, and spectral types between M4.0 and M4.5) and have been investigated spectroscopically earlier (Herbig & Rao 1972; Mathieu 1994; Wichmann et al. 1996; Kenyon et al. 1998; Scelsi et al. 2008; Sestito et al. 2008). The three of them displayed not only Hα in emission, but also Hβ and Hγ (we used one of them, J04393+335, in Fig. 3 to illustrate best the discarded wavelength ranges that are contaminated by activity in Sect. 3.2.2).

A large radius also translates into low gravity. Indeed, the brightest of the trio of T Tauri stars, J04313+241 AB (V927 Tau AB, $J = 9.73$ mag) was the only non-giant target with spectral index Ratio C < 1.07 (Fig. 6) and the only one to which we did not assign a luminosity class in Table A.3. Its optical spectrum is intermediate between those of giants and dwarfs of the same spectral type (M4.0:). Something similar is true for the other two T Tauri stars, which also have very low Ratio C indices for their spectral type (but all giant stars in our sample display

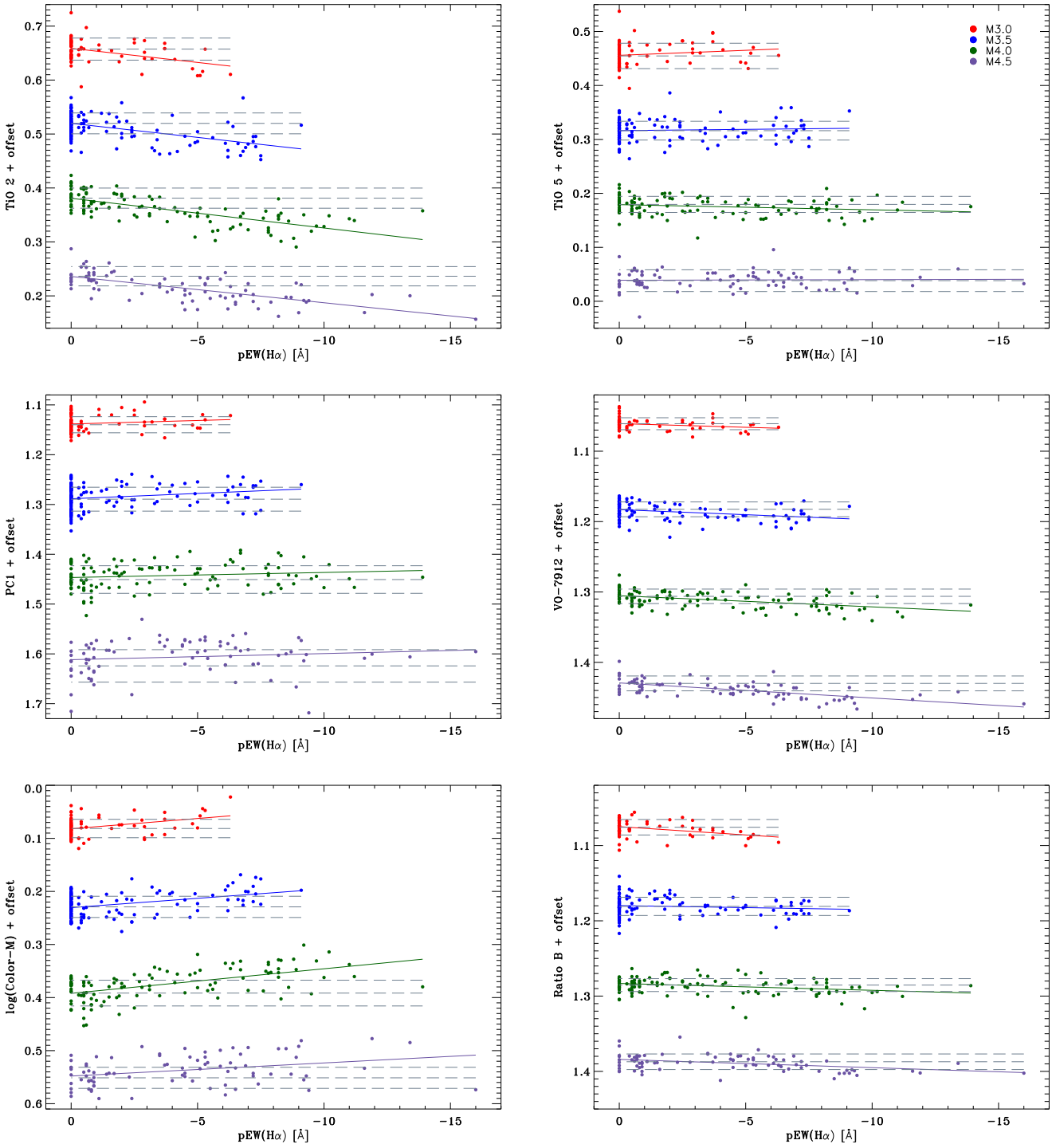

Fig. 9. Spectral-typing indices TiO 2, TiO 5 (*top*), PC1, VO-7912 (*middle*), Color-M, and Ratio B (*bottom*) as a function of Hα pseudo-equivalent width for spectral types M3.0 V, M3.5 V, M4.0 V, and M4.5 V, from top to bottom. For clarity, the indices are offset in steps of 0.1 in the vertical axis. Solid lines are linear fits of the indices as a function of $pEW(\alpha)$. Dashed lines indicate the mean and $\pm 1\sigma$ index at quiescence ($pEW(\alpha) > -1$ Å).

Hα in absorption). Although T Tauri stars are not natural targets for radial-velocity searches of low-mass exoplanets and none of the trio satisfies our criteria to be considered in the CARMENES sample (Table 1), a monitoring of bright, young, M dwarfs could shed light on the process of exoplanet formation (e.g., Crockett et al. 2012). Furthermore, young, nearby, very late stars are also ideal targets for direct-imaging surveys for Jupiter-like planetary companions at wide separations (Masciadri et al. 2005; Daemgen et al. 2007; Chauvin et al. 2010; Biller et al. 2013; Delorme et al. 2013, and references therein). Some of these targets are J13143+733 AB (NLTT 33370, M6.0 V in AB Doradus) and J09328+269 (DX Leo B, M5.5 V in Hercules-Lyra).

4.4.3. Effect of activity on spectral typing

As pointed out above, chromospheric activity could affect spectral typing. To study the validity of our results, we plot in Fig. 9 four of the five indices that we used for spectral typing as a function of $pEW(\mathrm{H}\alpha)$. We investigated the four spectral type intervals with the largest number of stars (in parenthesis): M3.0 V (72), M3.5 V (134), M4.0 V (113), and M4.5 V (84). Grouping by spectral type minimised the natural variation of the spectral index with effective temperature. The effect of activity on the TiO 5 and PC1 indices is not significant. However, strong activity in the largest quartile of $pEW(\mathrm{H}\alpha)$ has an appreciable effect on the indices VO-7912 and Color-M, but they fortuitously compensate each other because of the opposite slopes in their index vs. $pEW(\mathrm{H}\alpha)$ relations. The effect of activity on the TiO 2 index is more appreciable in the top left panel of Fig. 9, which agrees with the results shown by Hawley et al. (1996), who found that active M dwarfs tended to have lower values of TiO 2 (more absorption) than inactive dwarfs with the same TiO 5 indices (spectral types). However, this level of activity translates into a variation in spectral type of less than 0.8 subtypes for the most active stars, after using the coefficients in Table 5. In the end, the counter-weighting combination of five spectral indices and, especially, the use of the χ^2 and best-match methods guarantee that our adopted spectral types are free from the effect of chromospheric activity (for the investigated interval of $pEW(\mathrm{H}\alpha)$).

Our results on quantifying the variation of some spectral types as a function of activity are seemingly in contrast to some previous works, such as Morales et al. (2008). However, a direct comparison should be avoided because they grouped the stars by absolute magnitude, for which a determination of the distance is needed. A specific work on activity in M dwarfs will be another item of this series of papers on the science preparation of the CARMENES sample. It will be supported on one hand by new measurements of the emission of Hα, Hβ, and the Ca II H & K doublet and near-infrared triplet from high-resolution spectra and on the other hand by a comprehensive parallax distance compilation and accurate spectro-photometric distance determination.

5. Summary

CARMENES, the new spectrograph at the 3.5 m Calar Alto telescope, will spectroscopically monitor a sample of M dwarfs to detect exoplanets with the radial-velocity method. We are selecting the best planet host star candidates. For that, we are compiling a comprehensive list of dwarf stars coming from existing spectroscopic and photometric catalogues, as well as from late-type star studies. Currently, we are gathering all available information and determine fundamental properties from observations for approximately 2200 targets. Here we presented the first paper of a series that explains in detail the characterisation of our sample of targets for the CARMENES survey. This paper detailed optical low-resolution spectroscopy.

One of the key stellar astrophysical parameters that we need for each target is its spectral type. From the spectral type we estimate the stellar mass and infer planet detectability thresholds, and we ensure that we collate an even sampling of early-, mid-, and late-M dwarfs. Here, we undertook low-resolution spectroscopic observations of 753 targets with the CAFOS spectrograph on the 2.2 m Calar Alto telescope. This CAFOS sample contained M-dwarf candidates with poorly constrained spectral types, cool stars in multiple systems, and numerous comparison and standard stars. We classified our targets using both least-squares fitting techniques and 31 spectral indices, of which we chose five indices with small dispersion to empirically calibrate spectral types (TiO 2, TiO 5, PC1, VO-7912 and Color-M).

Additionally, we investigated the relation of spectral indices with surface gravity. We classified 25 of the observed targets as giant stars using the CaH series of related spectral indices, which are useful indicators to segregate giant stars from dwarfs. Metallicity was estimated through the ζ parameters (Lépine et al. 2007). We concluded that all our field dwarf stars except two new subdwarf candidates have solar metallicity. We identified 49 late-type stars as young dwarfs in star-forming regions or moving groups already reported in the bibliography.

Finally, we also computed stellar activity indicators. Stellar activity is a fundamental property for the CARMENES survey because activity features, such as photospheric spots, can mimic the signature of exoplanets or increase the stellar intrinsic jitter that can mask real exoplanet signals. We computed the pseudo-equivalent width of the Hα line of each target as an activity indicator, and analysed the effect of activity on spectral typing through indices. Although we have identified significant trends for some indices, the spectral type variation due to stellar activity is below one subtype level.

In summary, from the 753 targets that we observed with CAFOS, we obtained for the first time spectral types for 305 stars and improved it for 448 stars. We estimated gravity, metallicity, and activity indices for all targets. We identified 683 M dwarfs, of which 520 fulfill the CARMENES requirements and, therefore, will be included in the list of input targets. A more detailed investigation of these targets with high-resolution spectroscopic and imaging observations to select the best candidates for the CARMENES survey will produce the largest compilation of fully characterised M-type stars.

Acknowledgements. CARMENES is funded by the German Max-Planck-Gesellschaft (MPG), the Spanish Consejo Superior de Investigaciones Científicas (CSIC), the European Union through European Regional Fund (FEDER/ERF), the Spanish Ministry of Economy and Competitiveness, the state of Baden-Württemberg, the German Science Foundation (DFG), and the Junta de Andalucía, with additional contributions by the members of the CARMENES Consortium (Max-Planck-Institut für Astronomie, Instituto de Astrofísica de Andalucía, Landessternwarte Königstuhl, Institut de Ciències de l'Espai, Institut für Astrophysik Göttingen, Universidad Complutense de Madrid, Thüringer Landessternwarte Tautenburg, Instituto de Astrofísica de Canarias, Hamburger Sternwarte, Centro de Astrobiología, and the Centro Astronómico Hispano-Alemán). Financial support was also provided by the Universidad Complutense de Madrid, the Comunidad Autónoma de Madrid, the Spanish Ministerios de Ciencia e Innovación and of Economía y Competitividad, and the Fondo Europeo de Desarrollo Regional (FEDER/ERF) under grants AP2009-0187, SP2009/ESP-1496, AYA2011-30147-C03-01, -02, and -03, AYA2012-39612-C03-01, and ESP2013-48391-C4-1-R. Based on observations collected at the Centro Astronómico Hispano Alemán (CAHA) at Calar Alto, operated jointly by the Max–Planck Institut für Astronomie and the Instituto de Astrofísica de Andalucía. This research made use of the SIMBAD, operated at Centre de Données astronomiques de Strasbourg, France, the NASA's Astrophysics Data System, the RECONS project database (`http://www.recons.org`), the M, L, T, and Y dwarf compendium housed at `http://dwarfarchives.org` maintained by C. Gelino, J. D. Kirkpatrick and A. Burgasser, and the Washington Double Star Catalog maintained at the US Naval Observatory. We thank S. Lépine and E. Gaidos for sharing unpublished data with us, J. I. González-Hernández, E. W. Guenther, A. Hatzes, and M. R. Zapatero Osorio of the CARMENES Consortium for helpful comments, and the anonymous referee for the quick and encouraging report.

Appendix A: Long tables

Table A.1. Observed stars: identification, common name, Gliese number, 2MASS coordinates and J magnitude, observing date, and exposure time.

No.	Karmn	Name	Gl/GJ	α (J2000)	δ (J2000)	J [mag]	Observation date	$N \times t_{exp}$ [s]
1	J00066–070 AB	2MASS J00063925–0705354	...	00:06:39.20	–07:05:35.3	9.83	04 Aug. 2012	1×1000
2	J00077+603 AB	G 217–032	...	00:07:42.60	+60:22:54.3	8.91	24 Sep. 2012	1×600
3	J00115+591	LSR J0011+5908	...	00:11:31.82	+59:08:40.0	9.95	11 Jan. 2012	2×700
4	J00118+229	LP 348–40	...	00:11:53.03	+22:59:04.7	8.86	07 Dec. 2011	1×250
5	J00119+330	G 130–053	...	00:11:56.54	+33:03:17.8	9.07	07 Dec. 2011	1×220
6	J00122+304	1RXS J001213.6+302906	...	00:12:13.41	+30:28:44.3	10.24	12 Nov. 2011	1×600
7	J00133+275	[ACM2014] J0013+2733	...	00:13:19.52	+27:33:31.1	10.43	12 Nov. 2011	1×900
8	J00136+806	G 242–048	3014 A	00:13:38.71	+80:39:56.8	7.76	01 Sep. 2012	1×300
9	J00146+202	χ Peg	...	00:14:36.16	+20:12:24.1	1.76	11 Jan. 2012	1×1
10	J00152+530	G 217–040	...	00:15:14.53	+53:04:45.7	10.82	14 Feb. 2013	1×800

Notes. The full table is available at the CDS.

Table A.2. Seven representative spectral indices, ζ metallicity index, and Hα pseudo-equivalent width.

Karmn	PC1	TiO 2	TiO 5	VO-7912	Color-M	CaH 2	CaH 3	ζ	pEW(Hα) [Å]
J00066–070 AB	1.269	0.492	0.317	1.148	1.778	0.404	0.654	0.973	$-2.3^{+0.3}_{-0.5}$
J00077+603 AB	1.198	0.532	0.369	1.111	1.405	0.408	0.631	0.883	$-6.7^{+0.3}_{-0.4}$
J00115+591	1.511	0.378	0.202	1.222	2.902	0.281	0.564	0.970	$-1.6^{+0.2}_{-0.4}$
J00118+229	1.215	0.606	0.405	1.090	1.404	0.492	0.751	1.052	$-0.5^{+0.2}_{-0.2}$
J00119+330	1.167	0.634	0.427	1.072	1.293	0.503	0.748	1.023	$-0.3^{+0.1}_{-0.2}$
J00122+304	1.296	0.497	0.354	1.154	1.755	0.427	0.685	0.972	$-8.7^{+0.4}_{-0.5}$
J00133+275	1.296	0.512	0.339	1.144	1.805	0.425	0.686	0.994	$-4.0^{+0.2}_{-0.4}$
J00136+806	1.027	0.770	0.601	1.012	0.901	0.644	0.812	1.002	$+0.0^{+0.2}_{-0.2}$
J00146+202	0.955	0.729	0.520	1.005	0.643	0.839	0.946	2.754	$+0.8^{+0.1}_{-0.1}$
J00152+530	1.090	0.728	0.540	1.031	1.076	0.575	0.787	0.975	$+0.0^{+0.2}_{-0.2}$

Notes. The full table is available at the CDS.

Table A.3. Spectral types of observed stars.

Karmn	Sp. type biblio.	Ref.	Sp. type Best-fit	χ^2	Sp. type TiO2	TiO5	PC1	VO-7912	Color-M	Sp. type adopted
J00066–070 AB	M3.5 V+m4.5:	Reid07, Jan12	4.5	4.5	4.5	4.5	4.0	4.5	4.5	M4.5 V
J00077+603 AB	M4.5 V	Lep13	4.0	4.0	4.5	4.0	3.5	4.0	3.5	M4.0 V
J00115+591	M5.5 V	Lep03	6.0	6.0	5.5	6.0	5.5	5.5	5.5	M5.5 V
J00118+229	M3.5 V	Reid04	3.5	3.5	3.5	3.5	4.0	4.0	3.5	M3.5 V
J00119+330	M3.5 V	Giz97	3.5	3.0	3.5	3.5	3.5	3.5	3.5	M3.5 V
J00122+304	M5.0 V	Abe14	4.5	4.5	4.5	4.0	4.5	5.0	4.5	M4.5 V
J00133+275	M4.5 V	Abe14	4.5	4.5	4.5	4.5	4.5	4.5	4.5	M4.5 V
J00136+806	M1.5 V	PMSU	1.5	1.5	1.5	1.5	1.5	1.5	1.5	M1.5 V
J00146+202	M2 III	Gar89, Kir91	...	...	...	...	...	...	...	M III
J00152+530	M2.2 V	Mann13	2.5	2.0	2.5	2.0	2.5	2.0	2.5	M2.5 V

Notes. The full table is available at the CDS.

References. PMSU: Palomar/Michigan State University survey (see text); Simbad: spectral type as reported by Simbad; MP50: Moore & Paddock (1950); Vys56: Vyssotsky (1956); JM53: Johnson & Morgan (1953); Lee84: Lee (1984); Bid85: Bidelman (1985); Ste86: Stephenson (1986); SP88: Sanduleak & Pesch (1988); Gar89: García (1989); KMc89: Keenan & McNeil et al. (1989); Kir91: Kirkpatrick et al. (1991); Kri93: Krisciunas et al. (1993); Hen94: Henry et al. (1994); Jac94: Jacoby et al. (1994); Mar94: Martín et al. (1994); Giz97: Gizis (1997); GR97: Gizis & Reid (1997); Mot97: Motch et al. (1997); App98: Appenzeller et al. (1998); Gig98: Gigoyan et al. (1998); Mot98: Motch et al. (1998); Cut00: Cutispoto et al. (2000); Giz00: Gizis et al. (2000a); Li00: Li et al. (2000); CrRe02: Cruz & Reid (2002); Gray03: Gray et al. (2003); Lep03: Lépine et al. (2003); Reid03: Reid et al. (2003); Tee03: Teegarden et al. (2003); Reid04: Reid et al. (2004); Boc05: Bochanski et al. (2005); Scho05: Scholz et al. (2005); Gray06: Gray et al. (2006); Mon06: Montagnier et al. (2006); Riaz06: Riaz et al. (2006); SB06: Sánchez-Blázquez et al. (2006); Dae07: Daemgen et al. (2007); Eis07: Eisenbeiss et al. (2007); Reid07: Reid et al. (2007); BS08: Bender & Simon (2008); Jah08: Jahreiß et al. (2008); Law08: Law et al. (2008); LC08: López-Corredoira et al. (2008); Sce08: Scelsi et al. (2008); Cab09: Caballero (2009); Shk09: Shkolnik et al. (2009); Cab10: Caballero et al. (2010); Shk10: Shkolnik et al. (2010); LG11: Lépine & Gaidos (2011); Jan12: Janson et al. (2012); JE12: Jiménez-Esteban et al. (2012); RA12: Rojas-Ayala et al. (2012); Fri13: Frith et al. (2013); Lep13: Lépine et al. (2013); Mann13: Mann et al. (2013); Abe14: Aberasturi et al. (2014); Lam14: Lamert (2014); New14: Newton et al. (2014); RS14: Reyes-Sánchez (2014).

References

Aberasturi, M., Caballero, J. A., Montesinos, B., et al. 2014, AJ, 148, 36
Adibekyan, V. Zh., Sousa, S. G., Santos, N. C., et al. 2012, A&A, 545, A32
Allard, F., Homeier, D., & Freytag, B. 2011, ASP Conf. Ser., 448, 91
Allers, K. N., & Liu, M. C. 2013, ApJ, 772, 79
Alonso-Floriano, F. J., Caballero, J. A., & Montes, D. 2013a, Highlights of Spanish Astrophysics VII, 431
Alonso-Floriano, F. J., Montes, D., Jeffers, S. V., et al. 2013b, Protostars and Planets VI, 021
Amado, P. J., Quirrenbach, A., Caballero, J. A., et al. 2013, Highlights of Spanish Astrophysics VII, 842
Andersen, J. M., & Korhonen, H. 2015, MNRAS, 448, 3053
Appenzeller, I., Thiering, I., Zickgraf, F.-J., et al. 1998, ApJS, 117, 319
Artigau, É., Kouach, D., Donati, J.-F., et al. 2014, Proc. SPIE, 9147, E15
Avenhaus, H., Schmidt, H. M., & Meyer, M. R. 2012, A&A, 548, A105
Baraffe, I., Chabrier, G., Allard, F., & Hauschildt, P. H. 1998, A&A, 337, 403
Barnes, J. R., Jeffers, S. V., & Jones, H. R. A. 2011, MNRAS, 412, 1599
Barrado y Navascués, D. 1998, A&A, 339, 831
Barrado y Navascués, D., & Martín, E. L.2003, AJ, 126, 2997
Bean, J. L., Sneden, C., Hauschildt, P. H., Johns-Krull, C. M., & Benedict, G. F. 2006, ApJ, 652, 1604
Bean, J. L., Seifahrt, A., Hartman, H., et al. 2010, ApJ, 713, 410
Béjar, V. J. S., Gauza, B., Caballero, J. A., et al. 2012, 17th Cambridge Workshop on Cools Stars, Stellar Systems and the Sun, published on-line at http://www.coolstars17.net
Bender, C. F., & Simon, M. 2008, ApJ, 689, 416
Bensby, T., Feltzing, S., & Oey, M. S. 2014, A&A, 562, A71
Bergfors, C., Brandner, W., Janson, M., et al. 2010, A&A, 520, A54
Bidelman, W. P. 1985, ApJS, 59, 197
Biller, B. A., Liu, M. C., Wahhaj, Z., et al. 2013, ApJ, 777, 160
Bochanski, J. J., Hawley, S. L., Reid, I. N., et al. 2005, AJ, 130, 1871
Bochanski, J. J., West, A. A., Hawley, S. L., & Covey, K. R. 2007, AJ, 133, 531
Bonfils, X., Delfosse, X., Udry, S., et al. 2005, A&A, 442, 635
Bonfils, X., Mayor, M., Delfosse, X., et al. 2007, A&A, 474, 293
Bonfils, X., Delfosse, X.l, Udry, S., et al. 2013, A&A, 549, A109
Boyd, M. R., Winters, J. G., Henry, T. J., et al. 2011, AJ, 142, 10
Caballero, J. A. 2007, ApJ, 667, 520
Caballero, J. A. 2009, A&A, 507, 251
Caballero, J. A. 2010, A&A, 514, A98
Caballero, J. A. 2012, The Observatory, 132, 1
Caballero, J. A., Montes, D., Klutsch, A., et al. 2010, A&A, 520, A91
Caballero, J. A., Cortés-Contreras, M., López-Santiago, J., et al. 2013, Highlights of Spanish Astrophysics VII, 645
Casagrande, L., Flynn, C., & Bessell, M. 2008, MNRAS, 389, 585
Cayrel de Strobel, G., Soubiran, C., Friel, E. D., Ralite, N., & Francois, P. 1997, A&AS, 124, 299
Chabrier, G., Baraffe, I., Allard, F., & Hauschildt, P. 2000, ApJ, 542, 464
Chauvin, G., Lagrange, A.-M., Bonavita, M., et al. 2010, A&A, 509, A52
Cortés-Contreras, M., Caballero, J. A., Alonso-Floriano, F. J., et al. 2013, Highlights of Spanish Astrophysics VII, 646
Cortés-Contreras, M., Caballero, J. A., & Montes, D. 2014, The Observatory, 134, 348
Cortés-Contreras, M., Béjar, V. J. S., Caballero, J. A., et al. 2015, 18th Cambridge Workshop on Cools Stars, Stellar Systems and the Sun, in press
Crifo, F., Phan-Bao, N., Delfosse, X., et al. 2005, A&A, 441, 653
Crockett, C. J., Mahmud, N. I., Prato, L., et al. 2012, ApJ, 761, 164
Crossfield, I. J. M. 2014, A&A, 566, A130
Cruz, K. L., & Reid, I. N. 2002, AJ, 123, 2828
Cruz, K. L., Reid, I. N., Liebert, J., Kirkpatrick, J. D., & Lowrance, P. J. 2003, AJ, 126, 2421
Cruz, K. L., Reid, I. N., Kirkpatrick, J. D., et al. 2007, AJ, 133, 439
Cutispoto, G., Pastori, L., Guerrero, A., et al. 2000, A&A, 364, 205
Daemgen, S., Siegler, N., Reid, I. N., & Close, L. M. 2007, ApJ, 654, 558
da Silva, L., Torres, C. A. O., de La Reza, R., et al. 2009, A&A, 508, 833
Deacon, N. R., Liu, M. C., Magnier, E. A., et al. 2012, ApJ, 757, 100
Delfosse, X., Forveille, T., Beuzit, J.-L., et al. 1999, A&A, 344, 897
Delorme, P., Gagné, J., Girard, J. H., et al. 2013, A&A, 553, L5
Dhital, S., West, A. A., Stassun, K. G., & Bochanski, J. J. 2010, AJ, 139, 2566
Dhital, S., West, A. A., Stassun, K. G., et al. 2012, AJ, 143, 67
Dieterich, S. B., Henry, T. J., Jao, W.-C., et al. 2014, AJ, 147, 94
Dressing, C. D., & Charbonneau, D. 2013, ApJ, 767, 95
Dressing, C. D., & Charbonneau, D. 2015, ApJ, submitted [arXiv:1501.01623]
Ehrenreich, D., Lagrange, A.-M., Montagnier, G., et al. 2010, A&A, 523, A73
Eisenbeiss, T., Seifahrt, A., Mugrauer, M., et al. 2007, Astron. Nachr., 328, 521
Eisenbeiss, T., Ammler-von Eiff, M., Roell, T., et al. 2013, A&A, 556, A53
Fang, M. 2010, Ph.D. Thesis, Universität Heidelberg, Germany
Frith, J., Pinfield, D. J., Jones, H. R. A., et al. 2013, MNRAS, 435, 2161
Fuhrmeister, B., & Schmitt, J. H. M. M. 2003, A&A, 403, 247
Gagné, J., Lafrenière, D., Doyon, R., Malo, L., & Artigau, É. 2014, ApJ, 783, 121
Gaidos, E., & Mann, A. W. 2014, ApJ, 791, 54
Gaidos, E., Mann, A. W., Lépine, S., et al. 2014, MNRAS, 443, 2561
García, B. 1989, Bulletin d'Information du Centre de Données Stellaires, 36, 27
Gatewood, G., & Coban, L. 2009, AJ, 137, 402
Giclas, H. L., Slaughter, C. D., & Burnham, R. 1959, Lowell Observatory Bulletin, 4, 136
Giclas, H. L., Burnham, R., & Thomas, N. G. 1962, Lowell Observatory Bulletin, 5, 257
Gigoyan, K. S., Hambaryan, V. V., & Azzopardi, M. 1998, Astrophys., 41, 356
Gizis, J. E. 1997, AJ, 113, 806
Gizis, J. E., & Reid, I. N. 1997, PASP, 109, 1233
Gizis, J. E., & Reid, I. N. 2000, PASP, 112, 610
Gizis, J. E., Monet, D. G., Reid, I. N., et al. 2000a, MNRAS, 311, 385
Gizis, J. E., Monet, D. G., Reid, I. N., et al. 2000b, AJ, 120, 1085
Gizis, J. E., Reid, I. N., & Hawley, S. L. 2002, AJ, 123, 3356
Gliese, W., & Jahreiss, H. 1991, Preliminary Version of the Third Catalogue of Nearby Stars, NASA/Astronomical Data Center, Goddard Space Flight Center, Greenbelt
González, G. 1997, MNRAS, 285, 403
González Hernández, J. I., Rebolo, R., Israelian, G., et al. 2004, ApJ, 609, 988
Gould, A., & Chanamé, J. 2004, ApJS, 150, 455
Gray, R. O., Corbally, C. J., Garrison, R. F., McFadden, M. T., & Robinson, P. E. 2003, AJ, 126, 2048
Gray, R. O., & Corbally, C. J. 2009, Stellar Spectral Classification (Princeton University Press)
Gray, R. O., Corbally, C. J., Garrison, R. F., et al. 2006, AJ, 132, 161
Griffin, R. F., Griffin, R. E. M., Gunn, J. E., & Zimmerman, B. A. 1988, AJ, 96, 172
Guenther, E. W., & Tal-Or, L. 2010, A&A, 521, A83
Guenther, E. W., & Wuchterl, G. 2003, A&A, 401, 677
Hanson, R. B. 1975, AJ, 80, 379
Hawley, S. L., Gizis, J. E., & Reid, I. N. 1996, AJ, 112, 2799
Hawley, S. L., Covey, K. R., Knapp, G. R., et al. 2002, AJ, 123, 3409
Henry, T. J., Kirkpatrick, J. D., & Simons, D. A. 1994, AJ, 108, 1437
Henry, T. J., Walkowicz, L. M., Barto, T. C., & Golimowski, D. A. 2002, AJ, 123, 2002
Henry, T. J., Jao, W.-C., Subasavage, J. P., et al. 2006, AJ, 132, 2360
Herbig, G. H., & Rao, N. K. 1972, ApJ, 174, 401
Hidalgo, D. 2014, MSc Thesis, Universidad Complutense de Madrid, Spain
Holmberg, J., Nordström, B., & Andersen, J. 2009, A&A, 501, 941
Howard, A. W., Marcy, G. W., Bryson, S. T., et al. 2012, ApJS, 201, 15
Irwin, J., Berta, Z. K., Burke, C. J., et al. 2011, ApJ, 727, 56
Jacoby, G. H., Hunter, D. A., & Christian, C. A. 1984, ApJS, 56, 257
Jahreiß, H., Meusinger, H., Scholz, R.-D., & Stecklum, B. 2008, A&A, 484, 575
Jao, W.-C., Mason, B. D., Hartkopf, W. I., Henry, T. J., & Ramos, S. N. 2009, AJ, 137, 3800
Jao, W.-C., Henry, T. J., Subasavage, J. P., et al. 2011, AJ, 141, 117
Janson, M., Hormuth, F., Bergfors, C., et al. 2012, ApJ, 754, 44
Janson, M., Bergfors, C., Brandner, W., et al. 2014, ApJ, 789, 102
Jeffries, R. D. 1995, MNRAS, 273, 559
Jiménez-Esteban, F. M., Caballero, J. A., Dorda, R., Miles-Páez, P. A., & Solano, E. 2012, A&A, 539, A86
Jódar, E., Pérez-Garrido, A., Díaz-Sánchez, A., et al. 2013, MNRAS, 429, 859
Johnson, H. L., & Morgan, W. W. 1953, ApJ, 117, 313
Johnson, J. A., Aller, K. M., Howard, A. W., & Crepp, J. R. 2010, PASP, 122, 905
Joshi, M. M., Haberle, R. M., & Reynolds, R. T. 1997, Icarus, 129, 450
Joy, A. H., & Abt, H. A. 1974, ApJS, 28, 1
Kasting, J. F., Whitmire, D. P., & Reynolds, R. T. 1993, Icarus, 101, 108
Keenan, P. C., & McNeil, R. C. 1989, ApJS, 71, 245
Kenyon, S. J., Brown, D. I., Tout, C. A., & Berlind, P. 1998, AJ, 115, 2491
Kirkpatrick, J. D. 2005, ARA&A, 43, 195
Kirkpatrick, J. D., Henry, T. J., & McCarthy, D. W., Jr. 1991, ApJS, 77, 417
Kirkpatrick, J. D., Henry, T. J., & Simons, D. A. 1995, AJ, 109, 797
Kirkpatrick, J. D., Reid, I. N., Liebert, J., et al. 1999, ApJ, 519, 802

Klutsch, A., Alonso-Floriano, F. J., Caballero, J. A., et al. 2012, SF2A-2012: Proc. Annual meeting French Soc. Astron. Astrophys., 357
Klutsch, A., Freire Ferrero, R., Guillout, P., et al. 2014, A&A, 567, A52
Kopparapu, R. K. 2013, ApJ, 767, L8
Kopparapu, R. K., Ramírez, R., Kasting, J. F., et al. 2013, ApJ, 765, 131
Kotani, T., Tamura, M., Suto, H., et al. 2014, Proc. SPIE, 9147, E14
Krisciunas, K., Aspin, C., Geballe, T. R., et al. 1993, MNRAS, 263, 781
Lalitha, S., Czesla, S., Schmitt, J. H. M. M., et al. 2012, 17th Cambridge Workshop on Cools Stars, Stellar Systems and the Sun, published on-line at http://www.coolstars17.net
Lamert, A. 2014, MSc Thesis, Georg-August-Universität Göttingen, Germany
Lammer, H., Lichtenegger, H. I. M., Kulikov, Y. N., et al. 2007, Astrobiology, 7, 185
Law, N. M., Hodgkin, S. T., & Mackay, C. D. 2008, MNRAS, 384, 150
Lee, S.-G. 1984, AJ, 89, 702
Leggett, S. K., & Hawkins, M. R. S. 1988, MNRAS, 234, 1065
Lépine, S., & Gaidos, E. 2011, AJ, 142, 138
Lépine, S., & Shara, M. M. 2005, AJ, 129, 1483
Lépine, S., Rich, R. M., & Shara, M. M. 2003, AJ, 125, 1598
Lépine, S., Rich, R. M., & Shara, M. M. 2007, 669, 1235
Lépine, S., Thorstensen, J. R., Shara, M. M., & Rich, R. M. 2009, AJ, 137, 4109
Lépine, S., Hilton, E. J., Mann, A. W., et al. 2013, AJ, 145, 102
Li, J. Z., Hu, J. Y., & Chen, W. P. 2000, A&A, 356, 157
Lodieu, N., Scholz, R.-D., McCaughrean, M. J., et al. 2005, A&A, 440, 1061
Lodieu, N., Zapatero Osorio, M. R., & Martín, E. L. 2009, A&A, 499, 729
López-Corredoira, M., Gutiérrez, C. M., Mohan, V., Gunthardt, G. I., & Alonso, M. S. 2008, A&A, 480, 61
Magrini, L., Randich, S., Zoccali, M., et al. 2010, A&A, 523, A11
Mahadevan, S., Ramsey, L. W., Terrien, R., et al. 2014, Proc. SPIE, 9147
Maldonado, J., Martínez-Arnáiz, R. M., Eiroa, C., Montes, D., & Montesinos, B. 2010, A&A, 521, A12
Malo, L., Doyon, R., Lafrenière, D., et al. 2013, ApJ, 762, 88
Malo, L., Doyon, R., Feiden, G. A., et al. 2014, ApJ, 792, 37
Mamajek, E. E., Bartlett, J. L., Seifahrt, A., et al. 2013, AJ, 146, 154
Mann, A. W., Brewer, J. M., Gaidos, E., Lépine, S., & Hilton, E. J. 2013, AJ, 145, 52
Mann, A. W., Deacon, N. R., Gaidos, E., et al. 2014, AJ, 147, 160
Mann, A. W., Feiden, G. A., Gaidos, E., & Boyajian, T. 2015, ApJ, 804, 64
Martín, E. L., & Kun, M. 1996, A&AS, 116, 467
Martín, E. L., Rebolo, R., & Magazzù, A. 1994, ApJ, 436, 262
Martín, E. L., Rebolo, R., & Zapatero Osorio, M. R. 1996, ApJ, 469, 706
Martín, E. L., Delfosse, X., Basri, G., et al. 1999, AJ, 118, 2466
Masciadri, E., Mundt, R., Henning, T., Álvarez, C., & Barrado y Navascués, D. 2005, ApJ, 625, 1004
Mathieu, R. D. 1994, ARA&A, 32, 465
McWilliam, A. 1990, ApJS, 74, 1075
Meisenheimer, K. 1994, Sterne und Weltraum, 33, 516
Mochnacki, S. W., Gladders, M. D., Thomson, J. R., et al. 2002, AJ, 124, 2868
Montagnier, G., Ségransan, D., Beuzit, J.-L., et al. 2006, A&A, 460, L19
Montes, D., López-Santiago, J., Gálvez, M. C., et al. 2001, MNRAS, 328, 45
Montes, D., Alonso-Floriano, F. J., Tabernero, H. M., et al. 2013, Protostars and Planets VI, 2K022
Montes, D., Caballero, J. A., Alonso-Floriano, A. F., et al. 2015, 18th Cambridge Workshop on Cools Stars, Stellar Systems and the Sun, in press
Moore, J. H., & Paddock, G. F. 1950, ApJ, 112, 48
Morales, J. C., Ribas, I., & Jordi, C. 2008, A&A, 478, 507
Morales, J. C., Ribas, I., Caballero, J. A., et al. 2013, Highlights of Spanish Astrophysics VII, 664
Motch, C., Guillout, P., Haberl, F. , et al. 1997, A&A, 318, 111
Motch, C., Guillout, P., Haberl, F. , et al. 1998, A&AS, 132, 341
Mundt, R., Alonso-Floriano, F. J., Caballero, J. A., et al. 2013, Protostars and Planets VI, 2K055
Neves, V., Bonfils, X., Santos, N. C., et al. 2012, A&A, 538, A25
Neves, V., Bonfils, X., Santos, N. C., et al. 2013, A&A, 551, A36
Neves, V., Bonfils, X., Santos, N. C., et al. 2014, A&A, 568, A121
Newton, E. R., Charbonneau, D., Irwin, J., et al. 2014, AJ, 147, 20
Önehag, A., Heiter, U., Gustafsson, B., et al. 2012, A&A, 542, A33
Passegger, V.-M.. Wende, S., Reiners, A., et al. 2014, Towards other Earths II: the star-planet connection, in press
Pels, G., Oort, J. H., & Pels-Kluyver, H. A. 1975, A&A, 43, 423
Phan-Bao, N., & Bessell, M. S. 2006, A&A, 446, 515
Pickles, A., & Depagne, É. 2010, PASP, 122, 1437
Pounds, K. A., Allan, D. J., Barber, C., et al. 1993, MNRAS, 260, 77
Poveda, A., Herrera, M. A., Allen, C., Cordero, G., & Lavalley, C. 1994, Rev. Mex. Astron. Astrophys., 28, 43
Quirrenbach, A., Amado, P. J., Mandel, H., et al. 2010, Proc. SPIE, 7735, E13
Quirrenbach, A., Amado, P. J., Seifert, W., et al. 2012, Proc. SPIE, 8446
Quirrenbach, A., Amado, P. J., Caballero, J. A., et al. 2014, Proc. SPIE, 9147, E1F
Rajpurohit, A. S., Reylé, C., Allard, F., et al. 2013, A&A, 556, A15
Rajpurohit, A. S., Reylé, C., Allard, F., et al. 2014, A&A, 564, A90
Recio-Blanco, A., Bijaoui, A., & de Laverny, P. 2006, MNRAS, 370, 141
Reid, N. 1992, MNRAS, 257, 257
Reid, N. 1993, MNRAS, 265, 785
Reid, I. N., Hawley, S. L., & Gizis, J. E. 1995, AJ, 110, 1838
Reid, I. N., Gizis, J. E., & Hawley, S. L. 2002, AJ, 124, 2721
Reid, I. N., Cruz, K. L., Allen, P., et al. 2003, AJ, 126, 3007
Reid, I. N., Cruz, K. L., Allen, P., et al. 2004, AJ, 128, 463
Reid, I. N., Cruz, K. L., & Allen, P. 2007, AJ, 133, 2825
Reid, I. N., Cruz, K. L., Kirkpatrick, J. D., et al. 2008, AJ, 136, 1290
Reiners, A., & Basri, G. 2009, ApJ, 705, 1416
Reiners, A., & Basri, G. 2010, ApJ, 710, 924
Reiners, A., Bean, J. L., Huber, K. F., et al. 2010, ApJ, 710, 432
Reiners, A., Shulyak, D., Anglada-Escudé, G., et al. 2013, A&A, 552, A103
Reyes-Sánchez, K. P. 2014, MSc Thesis, Universidad Internacional de Valencia, Spain
Reylé, C., Scholz, R.-D., Schultheis, M., Robin, A. C., & Irwin, M. 2006, MNRAS, 373, 705
Riaz, B., Gizis, J. E., & Harvin, J. 2006, AJ, 132, 866
Riaz, B., Gizis, J. E., & Samaddar, D. 2008, ApJ, 672, 115
Ribas, I. 2003, A&A, 400, 297
Riddick, F. C., Roche, P. F., & Lucas, P. W. 2007, MNRAS, 381, 1067
Ridgway, S. T., Joyce, R. R., White, N. M., & Wing, R. F. 1980, ApJ, 235, 126
Riedel, A. R., Finch, C. T., Henry, T. J., et al. 2014, AJ, 147, 85
Robertson, P., Endl, M., Henry, G. W., et al. 2015, ApJ, 801, 79
Rodríguez-López, C., Anglada-Escudé, G., Amado, P. J., et al. 2014, Highlights of Spanish Astrophysics VIII, in press
Rojas-Ayala, B., Covey, K. R., Muirhead, P. S., & Lloyd, J. P. 2010, ApJ, 720, L113
Rojas-Ayala, B., Covey, K. R., Muirhead, P. S., & Lloyd, J. P. 2012, ApJ, 748, 93
Sánchez, S. F., Aceituno, J., Thiele, U., Pérez-Ramírez, D., & Alves, J. 2007, PASP, 119, 118
Sánchez, S. F., Thiele, U., Aceituno, J., et al. 2008, PASP, 120, 1244
Sánchez-Blázquez, P., Peletier, R. F., Jiménez-Vicente, J., et al. 2006, MNRAS, 371, 703
Sandage, A. 1969, ApJ, 158, 1115
Sandage, A., & Kowal, C. 1986, AJ, 91, 1140
Sanduleak, N., & Pesch, P. 1988, ApJS, 66, 387
Scalo, J., Kaltenegger, L., Segura, A. G., et al. 2007, Astrobiology, 7, 85
Scelsi, L., Maggio, A., Michela, G., et al. 2007, A&A, 468, 405
Scelsi, L., Sacco, G., Affer, L., et al. 2008, A&A, 490, 601
Schlaufman, K. C., & Laughlin, G. 2010, A&A, 519, A105
Schlieder, J. E., Lépine, S., & Simon, M. 2012a, AJ, 143, 80
Schlieder, J., Lépine, S., Rice, E., et al. 2012b, AJ, 143, 114
Schlieder, J., Bonnefoy, M., Herbst, T. M., et al. 2014, ApJ, 783, 27
Scholz, R.-D., Meusinger, H., & Jahreiß, H. 2005, A&A, 442, 211
Seeliger, M., Neuhäuser, R., & Eisenbeiss, T. 2011, AN, 332, 821
Seifert, W., Sánchez Carrasco, M. A., Xu, W., et al. 2012, Proc. SPIE, 8446, E33
Sestito, P., Palla, F., & Randich, S. 2008, A&A, 487, 965
Shkolnik, E., Liu, M. C., & Reid, I. N. 2009, ApJ, 699, 649
Shkolnik, E. L., Hebb, L., Liu, M. C., Reid, I. N., & Collier Cameron, A., 2010, ApJ, 716, 1522
Shkolnik, E. L., Anglada-Escudé, G., Liu, M. C., et al. 2012, ApJ, 758, 56
Shulyak, D., Seifahrt, A., Reiners, A., Kochukhov, O., & Piskunov, N. 2011, MNRAS, 418, 2548
Skrutskie, M. F., Cutri, R. M., Stiening, R., et al. 2006, AJ, 131, 1163
Sousa, S. G., Santos, N. C., Mayor, M., et al. 2008, A&A, 487, 373
Sousa, S. G., Santos, N. C., Israelian, G., Mayor, M., & Udry, S. 2011, A&A, 533, A141
Stauffer, J. R., & Hartmann, L. W. 1986, ApJS, 61, 531
Stauffer, J. R., Giampapa, M. S., Herbst, W., et al. 1991, ApJ, 374, 142
Stephenson, C. B. 1986, AJ, 91, 144
Strom, S. E., & Strom, K. M. 1967, ApJ, 150, 501
Tabernero, H. M., Montes, D., & González Hernández, J. I. 2012, A&A, 547, A13
Tabernero, H. M., Montes, D., González Hernández, J. I., & Ammler-von Eiff, M. 2015, A&A, in press [arXiv:1409.2348]
Tarter, J. C., Backus, P. R., Mancinelli, R. L., et al. 2007, Astrobiology, 7, 30
Teegarden, B. J., Pravdo, S. H., Hicks, M., et al. 2003, ApJ, 589, L51
Terrien, R. C., Mahadevan, S., Bender, C. F., et al. 2012, ApJ, 747, L38
Tokovinin, A. 2008, MNRAS, 389, 925
Torres, C. A. O., Quast, G. R., Melo, C. H. F., & Sterzik, M. F. 2008, in Handbook of Star Forming Regions, Volume II, 757

Tsuji, T., & Nakajima, T. 2014, PASJ, 66, 98
Valenti, J. A., & Fischer, D. A. 2005, ApJS, 159, 141
Valenti, J. A., & Piskunov, N. 1996, A&AS, 118, 595
van Altena, W. F. 1966, AJ, 71, 482
van Maanen, A. 1945, ApJ, 102, 26
Vyssotsky, A. N. 1956, AJ, 61, 201
West, A. A., Hawley, S. L., Walkowicz, L. M., et al. 2004, AJ, 128, 426
West, A. A., Morgan, D. P., Bochanski, J. J., et al. 2011, AJ, 141, 97
White, R., & Basri, G. 2003, ApJ, 582, 1109
Wichmann, R., Krautter, J., Schmitt, J. H. M. M., et al. 1996, A&A, 312, 439
Wilking, B. A., Meyer, M. R., Robinson, J. G., & Greene, T. P. 2005, AJ, 130, 1733
Winters, J. G., Henry, T. J., Lurie, J. C., et al. 2015, AJ, 149, 5
Woolf, V. M., & Wallerstein, G. 2005, MNRAS, 356, 963
Woolf, V. M., & Wallerstein, G. 2006, PASP, 118, 218
Woolf, V. M., Lépine, S., & Wallerstein, G. 2009, PASP, 121, 117
Xing, L.-F., & Xing, Q.-F. 2012, A&A, 537, A91
Yi, Z., Luo, A., Song, Y., et al. 2014, AJ, 147, 33
Zboril, M., & Byrne, P. B. 1998, MNRAS, 299, 753
Zechmeister, M., Kürster, M., & Endl, M. 2009, A&A, 505, 859
Zechmeister, M., Kürster, M., Endl, M., et al. 2013, A&A, 552, A78
Zuckerman, B., & Song, I. 2004, ARA&A, 42, 685
Zuckerman, B., Song, I., & Bessell, M. S. 2004, ApJ, 613, L65
Zuckerman, B., Vican, L., Song, I., & Schneider, A. 2013, ApJ, 778, 5